Nanooptics with anisotropic 2D materials

Pablo Alonso González[1,2]

[1]Department of Physics, University of Oviedo, Oviedo 33006, Spain.
[2]Center of Research on Nanomaterials and Nanotechnology, CINN (CSIC--Universidad de Oviedo), El Entrego 33940, Spain.
E-mail: pabloalonso@uniovi.es

Highly anisotropic crystals have recently attracted considerable attention because of their ability to support polaritons with a variety of unique properties, such as hyperbolic dispersion, negative phase velocity, or extreme field confinement. In particular, the biaxial van der Waals semiconductors α-phase molybdenum trioxide (α-MoO_3) and vanadium pentaoxide (V_2O_5) have received attention due to their ability to support in-plane hyperbolic phonon polaritons[1-3] (PhPs) —infrared (IR) light coupled to lattice vibrations in polar materials—, offering an unprecedented platform for studying and controlling the flow of energy at the nanoscale.

Here, we will show experimental demonstrations of the unique behaviour of PhPs in these crystals including highly directional propagation (Fig. 1, left panel), natural waveguiding (Fig.1, middle panel)[4-7], anomalous refraction (Fig.1, right panel)[8], and negative reflection[9].

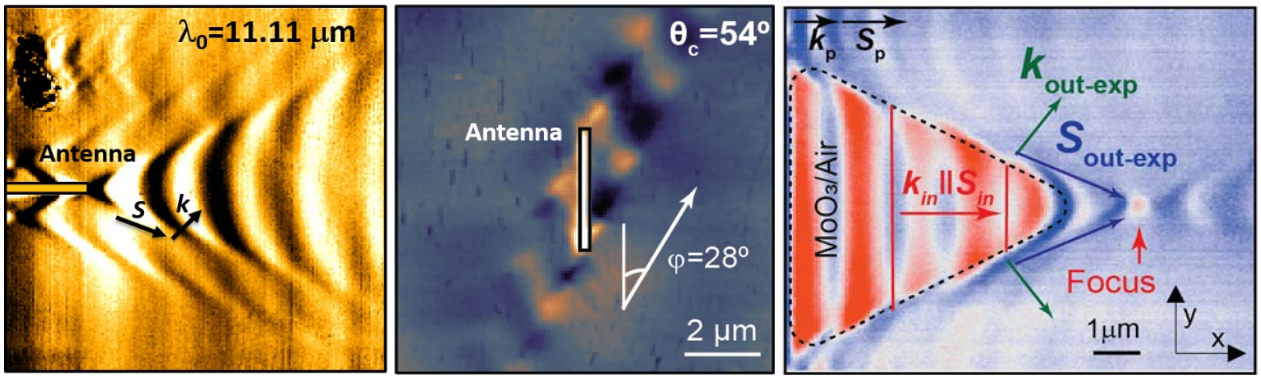

Fig. 1 . Left: real-space image of hyperbolic PhPs propagating in an α-MoO_3 slab. Middle: real-space image of PhPs being canalized (unidirectional propagation) in a twisted bi-layered α-MoO_3 structure. Right: real-space image of anomalous refraction of PhPs in α-MoO_3.

References

[1] W. Ma et al., *Nature* **562**, 557 (2018).
[2] J. Taboada-Gutiérrez et al., *Nat. Mater.* (2020). https://doi.org/10.1038/s41563-020-0665-0
[3] G. Álvarez-Pérez et al., *Adv. Mater.* **32**, 1908176 (2020).
[4] J. Duan et al., *Nano Lett.* (2020).
[5] G.Hu et al., *Nature* **582**, 209 (2020).
[6] M. Chen, et al.,*Nature Materials* (2020).
[7] Z. Zheng et al., *Nano Lett*. **20**, 7, 5301-5308 (2020).
[8] J. Duan et al., *Nat. Comm*. 12, 1, 1-8 (2021).
[9] G. Álvarez-Pérez et al., *arXiv:2202.13877* (2022).

Controlling the dynamical photonic properties of phonon-polaritons in two-dimensional crystals by engineering dielectric-metallic substrates

Francisco C. B. Maia[1], Flávio H. Feres[1, 2], Rafael A. Mayer[1, 3], Ingrid D. Barcelos[1] and Raul de O. Freitas[1]

1. Brazilian Synchrotron Light Laboratory (LNLS), Brazilian Center for Research in Energy and Materials (CNPEM), Zip Code 13083-970, Campinas, Sao Paulo, Brazil.
2. Physics Department, Institute of Geosciences and Exact Sciences, São Paulo State University – UNESP, Rio Claro 13506-900, Brazil
3. Physics Department, Gleb Wataghin Physics Institute, University of Campinas (Unicamp), 13083-859 Campinas, Sao Paulo, Brazil
E-mail: francisco.maia@lnls.br

To control light-matter interactions at the nanoscale, like polaritons in two-dimensional (2D) crystals [1], is a prime goal in nanophotonics. Here we use synchrotron infrared nanospectroscopy (SINS) to demonstrate group velocity modulation [2] of subwavelength hyperbolic phonon-polariton waves, propagating in a 2D hexagonal boron nitride (hBN) crystal lying on a SiO_2/Au substrate (Fig. 1a), as a function of the SiO_2 film thickness, **d**. In quantitative agreement with our theoretical predictions, we observe that the polariton group velocity value notably increases from ~ 1.8×10^6 m.s^{-1} to ~ 4.8×10^6 m.s^{-1} as **d** varies from 0 to 300 nm (Fig. 1a). Underpinned on such insightful observation, we simulate the polaritonic pulse dynamics for a layered heterostructure with a SiO_2 thickness gradient consisting of a hBN crystal lying on a SiO_2 wedge etched in Au (Fig. 1b). For a same timeframe, we note that the pulse propagates faster in the hBN/SiO_2-wedge/Au (Fig. 1c-e) compared to that in hBN/Au (Fig. 1f-h). In contrast to the linear temporal displacement of the pulse on hBN/Au (crosses), we see a non-linear behavior (circles) for the wedge case. Using a semi-quantum approach considering polaritonic pulse as free particle possessing effective mass depending on the group velocity, we derive an equation of motion that not only explains the pulse dynamics either on the wedge and on Au (curves in Fig. 1i) but also allows for predicting its acceleration (Fig. 1j). Our work, therefore, reveals fundamental details on the semi-quantum behavior of the polaritons in 2D crystals. Moreover, we show that metallic-dielectric functional substrates can be designed to control the dynamics of subwavelength polaritons that is highly desirable for polaritonic devices.

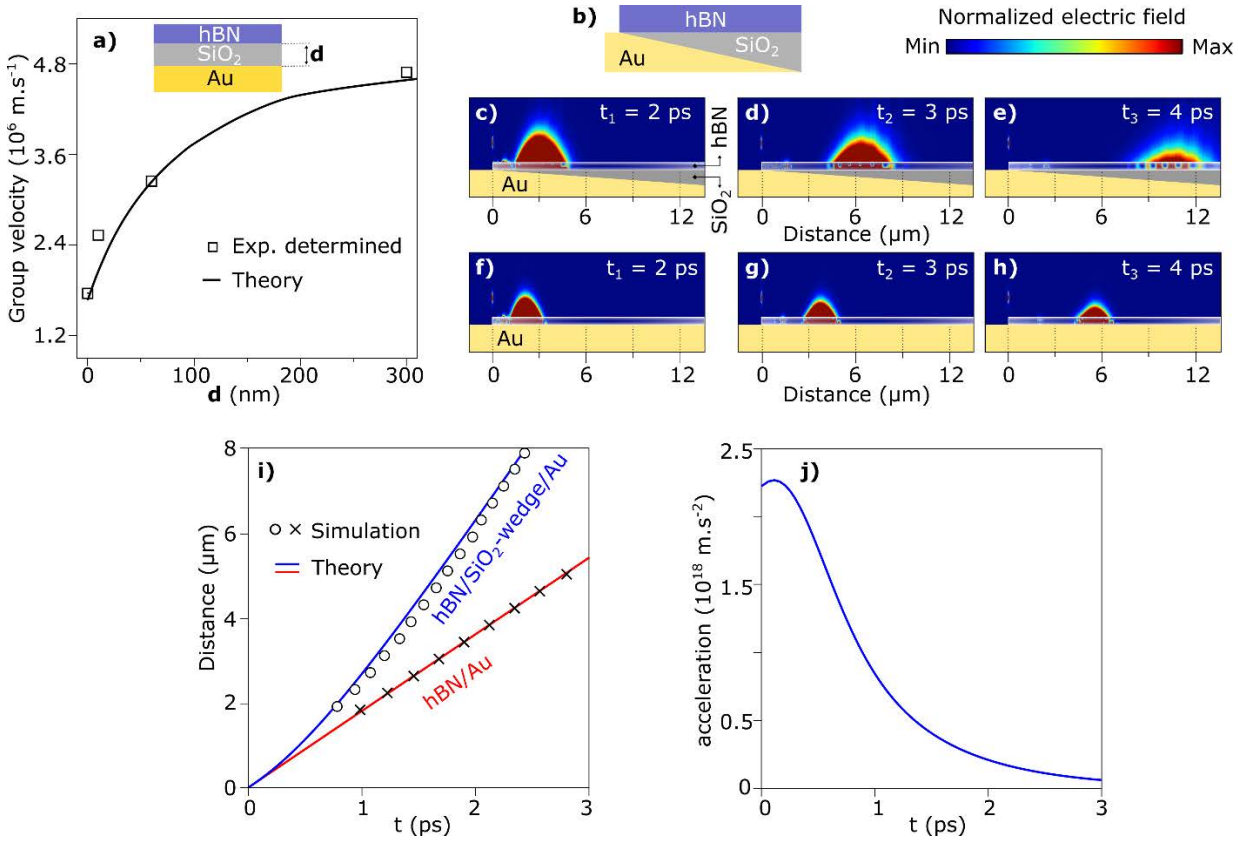

Fig. 1 (a) Polariton group velocity modulation as a function of the SiO_2 thickness. (b) hBN/SiO_2-wedge/Au scheme. Propagation of the polariton pulse in the hBN/SiO_2-wedge/Au heterostructure (c-e) and in hBN/Au (f-h). (i) Simulated and theoretical temporal displacement of the pulse for the two considered systems. (j) Theoretically predicted acceleration by the semi-quantum modelling. These figures were adapted from ref. [2].

References

1. Low, T.; Chaves, A.; Caldwell, J. D.; Kumar, A.; Fang, N. X.; Avouris, P.; Heinz, T. F.; Guinea, F.; Martin-Moreno, L. and Koppens, F. 2016. *Nature Materials*, 16, 182-194.
2. Feres, F.; Mayer, R. A.; Barcelos, I. D.; Freitas, R. O. and Maia, F. C. B. 2020. *ACS Photonics*, 7, 1396-1402.

Interrogating Single Molecule Kinetics of Citrate Synthase with Plasmonic Optical Tweezers

Edona Karakaçi,[1] **Cuifeng Ying,**[1,2] **Alessandro Ianiro,**[1] **Esteban Bermúdez-Ureña,**[1,3] **Reuven Gordon,**[4] **Michael Mayer**[1]

1. Adolphe Merkle Institute, University of Fribourg, Chemin des Verdiers 4, CH-1700 Fribourg, Switzerland.
2. Advanced Optics and Photonics Lab, Department of Engineering, Nottingham Trent University, United Kingdom.
3.Centro de investigación en Ciencia e Ingeniería de Materiales and Escuela de Física, Universidad de Costa Rica, San José, 11501, Costa Rica
4. Department of Electrical and Computer Engineering, University of Victoria, Victoria, British Columbia V8P 5C2, Canada

Email: edona.karakaci@unifr.ch

Studying conformational dynamics of label-free single proteins is essential to fully understand their function. Ensemble measurements for analyzing protein dynamics are limited to averaged information from a protein population, and are unable to capture heterogeneity with regards to post-translational modifications, folding states, mutations or other variations. Existing single-molecule techniques for determining conformational changes of proteins in real time, require labeling or other modifications, which can alter the native state and function of the protein under observation. Here we present an approach that makes it possible to monitor a single unmodified protein trapped in a plasmonic hotspot [1-2] with a temporal resolution of 40 microseconds.[3] To demonstrate that plasmonic optical tweezers can reveal insights into the conformational dynamics of native proteins that so far have not been investigated on a single molecule level, we examined citrate synthase (molecular mass: 98 kDa). This enzyme of the Krebs cycle catalyzes the condensation of oxaloacetate (OAA) and acetyl coenzyme A (AcCoA) to citrate and coenzyme A and consists of two identical subunits with one active site per subunit.[4-5] During catalysis, each subunit independently closes upon substrate binding and opens for product release and renewed substrate binding.[5] We show that programmable fluidics made it possible to monitor conformational changes of citrate synthase in response to different substrate concentrations or inhibitors for hours.[3] The approach reveals that during the enzymatic cycle, the subunits of citrate synthase populate a previously unknown, intermediate conformation that is crucial for enzyme activity (Fig.1).[3]

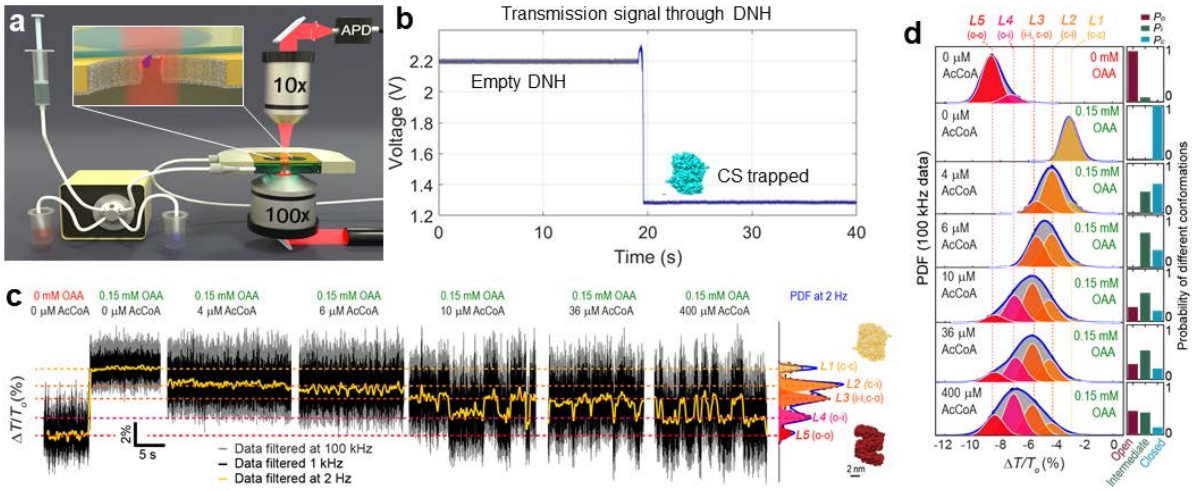

Fig. 1 Conformational dynamics of single Citrate Synthase (CS) enzymes as a function of substrate concentration.[3] **a**, Schematic illustration of a plasmonic optical tweezer platform. A linearly polarized laser (λ = 852 nm) was focused on a double nanohole (DNH) structure on a silica wafer and the transmitted light was detected with an avalanche photodiode (APD). The inset illustrates a trapped protein (blue) near the plasmonic hotspot (pink) of a DNH structure in the focal point. **b**, Transmission time trace for a CS protein being trapped experimentally in a DNH structure. **c**, Normalized transmission recordings of a single CS protein trapped in the DNH first in the absence of substrates and then in the presence of a constant OAA concentration and increasing AcCoA concentrations. The probability density function (PDF) on the right was calculated from all transmission traces after low-pass filtering at 2 Hz. Dashed lines in five different colors are centered at the peaks of the PDF, representing five conformational states of dimeric CS. **d**, Change in the occupancy of transmission levels L1 to L5 (indicated in panel **c**) as a function of substrate concentration and corresponding probabilities of the open state *Po*, intermediate state *Pi*, and closed state *Pc* of the subunits of CS.[3]

References

[1] Juan, M. L.; Gordon, R.; Pang, Y.; Eftekhari, F.; Quidant, R. 2009, *Nat. Phys.* 5, 915–919
[2] Pang, Y.; Gordon, R. 2012, *Nano Lett.* 12, 402–406.
[3] Ying, C.; Karakaci, E.; Bermudez-Urena, E.; Ianiro, A.; Foster, C.; Awasthi, S.; Guha, A.; Bryan, L.; List, J.; Balog, S. 2021, *arXiv Prepr*, arXiv2107.06407.
[4] Srere, P. A. 1972, Curr. Top. *Cell. Regul.* 5, 229–283.
[5] Remington, S. J 1992, Curr. Top. *Cell. Regul.* 33, 209–229.

Efficient optically-driven nanomotor designed by deep learning

Mintae Chung, Karim Achouri and Olivier J.F. Martin

Nanophotonics and Metrology Laboratory, Swiss Federal Institute of Technology Lausanne (EPFL), Switzerland

E-mail: olivier.martin@epfl.ch

We present nanomotors built from a 200 nm plasmonic rotor – Fig. 1(a) – embedded into a 2 μm SiO_2 body, Fig. 1(b). The shape of the plasmonic rotor was optimized using deep learning to produce a strong torque upon linear polarized illumination. Using images from the rotor, we applied a convolutional neural network connected to a deep convolution generative adversarial network to devise geometries that would exhibit a strong torque. With this procedure, we were able to discover rotor geometries that exhibited a torque one order of magnitude larger than those in the initial training set. Some of the most promising nanostructures were then fabricated using a relatively complex process that included ion beam etching of the plasmonic rotor, followed by embodiment in SiO2. The sub-20 nm features of the rotor required a careful optimization of the electron beam lithography and of the ion beam etching. In spite of these multiple steps, the yield of this technology was quite high and arrays of nanomotors were fabricated this was, Fig. 1(b). Finally, the nano-motors were detached from their substrate using a sacrificial layer and transferred into the fluidic experiment chamber for measurements. Near-field calculations were applied to understand the origin of the rotation under linear polarization illumination, Fig. 1(c). It turns out that the torque exhibited by those structures takes its origin in the conjoint action of a pair of multipoles. Rapid rotation speeds were observed experimentally under linear polarized illumination, Fig. 1(d).

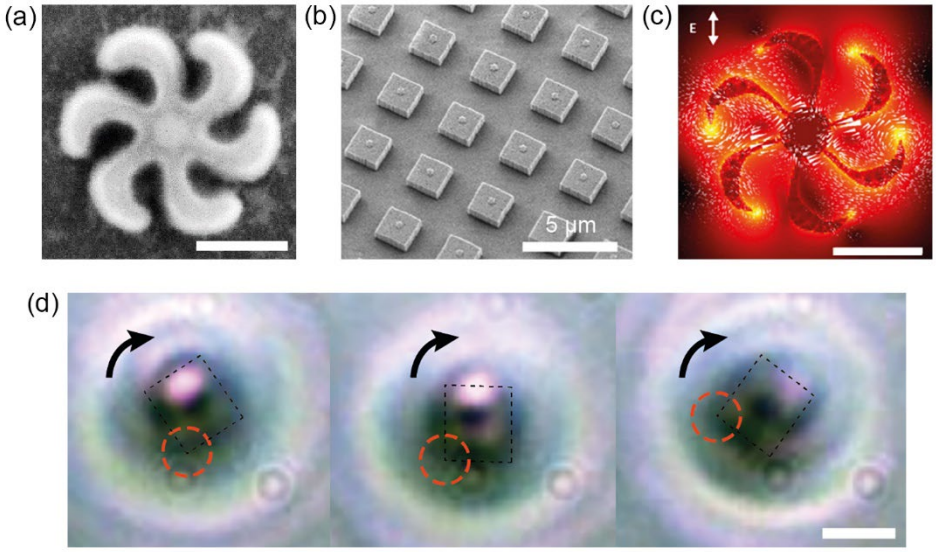

Fig. 1 Nanomotors presented in this work. (a) The shape of the plasmonic rotor was optimized using machine learning to produce the strongest torque possible under linear illumination (scalebar 100 nm). The rotor was fabricated using electron beam lithography and ion etching [1]. (b) The rotor was then embedded into an SiO_2 body. A very high yield was obtained with thousands of nanomotors fabricated on the same wafer. (c) The origin of the torque experienced by the rotor under linear illumination can be traced back to its near-field and stems from the interaction of a pairs of dipoles (scalebar 100 nm). (d) Successive snapshots of the nanomotor demonstrating its rapid rotation under linear illumination (scalebar 1 μm).

Reference

[1] Abasahl, A, Santschi, Ch, Raziman, TV, Martin, OJF. 2021. *Nanotechnology*, **32**, 475202 (2021).

Optical Manipulation of Matter Waves

Kamran Akbari[1], **Valerio Di Giulio**[1], **F. Javier García de Abajo**[2]

1. ICFO-Institut de Ciencies Fotoniques, The Barcelona Institute of Science and Technology, 08860 Castelldefels (Barcelona), Spain

2. ICREA-Institució Catalana de Recerca i Estudis Avançats, Passeig Lluis Companys 23, 08010 Barcelona, Spain
E-mail: kamran.akbari@icfo.eu

Light is used to drive excitations in atoms, molecules, and matter in general. Additionally, it is extensively employed to trap atoms, molecules, particles, and living cells, as well as to steer their motion in the context of atomic and molecular optics. Likewise, light can be also used to steer electrons through elastic ponderomotive interactions. More strikingly, light-electron inelastic interaction has emerged as a powerful way to manipulate electrons as probes, enabling an unprecedented combination of energy, space, and now also time resolution in the field of ultrafast electron microscopy. This allows one to investigate fast dynamics of structural changes in the picosecond range and electronic motion in the femtosecond range, particularly through the technique that has become widely known as photon-induced near-field electron microscopy (PINEM) [1]. Specifically, electron-light interaction can take place via either direct coupling of the linear field term in the interaction Hamiltonian or pondermotive coupling assisted by the quadratic field term. Interactions due to ponderomotive forces can modulate the transverse wave function, producing diffraction (Kapitza-Dirac effect) that has been suggested as a way to shape electron focal spots and correct aberrations [2]. However, electron-light interaction in free space is rather weak.

In this work, we propose configurations to control the translational motion of atoms and molecules in a similar way as done for electrons in PINEM (Fig. 1), with the advantage that the interaction can be made stronger. Besides its fundamental interest in the extension of such interactions from electrons to atoms, we foresee practical application in the creation of temporally compressed atom waves, similar to electron pulse compression in PINEM. In addition, we anticipate a new form of photon-induced near-field atom microscopy (PINAM), in which atoms instead of electrons are used to probe localized excitations, providing stronger interaction with light, particularly when the light is tuned close to an atomic resonance, together with a richer scenario in which the internal state of the probe can play a role.

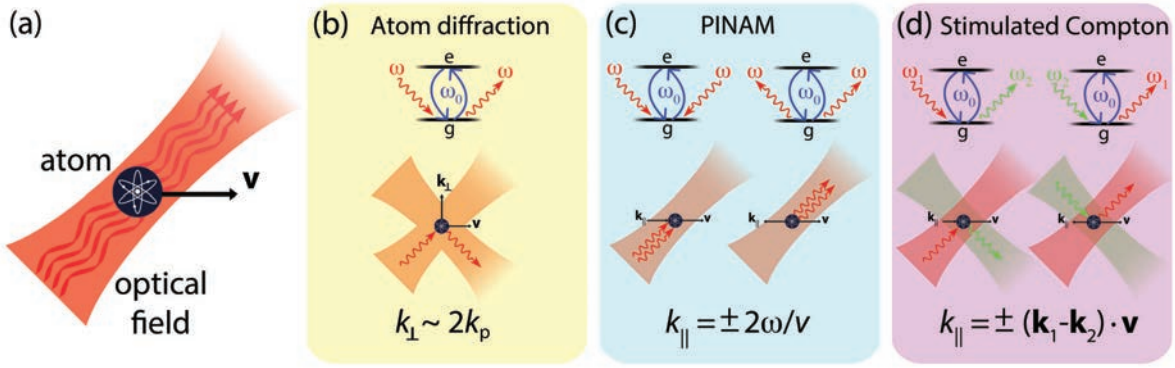

Fig. 1 Interaction of a neutral atom with optical fields. (a) Various appealing configurations are feasible by leveraging the interaction of a moving atom with optical fields shown in the panel. The atom is initially in its internal ground state, where the first excited state has the energy difference of $\hbar\omega_0$. (b) Diffraction of an atom by alight classical field is the most probable outcome, in which there is no exchange of real photons, so that the momentum change is only in the transverse direction. (c) Photon-induced near-field atom microscopy (PINAM) constitutes another interesting possibility enabling by atom-field interaction, in which an even number of photons need to be exchanged, and hence, the longitudinal momentum of the atom is altered by the kicks associated to them. (d) Stimulated Compton scattering of a moving atom in the field of two laser beams with frequencies ω_1 and ω_2 also appears to be feasible. In it, the atom absorbs a photon from one of the beams and emits another photon to the other beam. This results in a change in the longitudinal momentum.

References

[1] Park S T, Lin M, Zewail A H, 2010, *New J. Phys.* 12, 123028.
[2] García de Abajo F J, Di Giulio V, 2021, *ACS Photonics* 8, 945-974.

Plasmonic nano-optical tweezers towards single quantum dots trapping

Quanbo Jiang,[1,2] Jean-Benoît Claude, [2] Benoît Rogez,[2] Prithu Roy, [2] Guillaume Baffou,[2] Jérôme Wenger[2]

1. Light, Nanomaterials, Nanotechnologies (L2n), Institut Charles Delaunay, CNRS, Université de Technologie de Troyes, 10004 Troyes, France
2. Aix Marseille Univ, CNRS, Centrale Marseille, Institut Fresnel, AMUTech, 13013 Marseille, France

quanbo.jiang@utt.fr

Gold nanoapertures or nanoantennas can generate strong field gradients enabling efficient optical trapping of nano-objects [1,2]. Thanks to the accurate nanoscale positioning of plasmonic optical tweezers, trapping single quantum emitters such as NV centers, quantum dots or nanocrystals becomes a trend for single photon sources. However, many factors such as local temperature increase, thermophoretic force or photoblinking all affect this delicate experiment.

Here, we use plasmonic nanoantennas to simultaneously trap single colloidal quantum dots and enhance their photoluminescence (Fig. 1a). The nanoantennas are milled in the gold film and designed to generate an extremely high electric field in the gap (Fig. 1b). First, as the infrared trapping beam is also partly absorbed into the metal, Joule heating leads to a local temperature increase [3,4] which requires proper calibration and measurement as it may affect the trapping potential. We develop a method to measure the local temperature in the trap based on the fluorescence of Alexa fluor dyes under the trapping condition [5]. Second, a temperature gradient is present around the plasmonic nano-tweezers, leading to an additional thermophoretic force. We demonstrate that the surfactant sodium dodecyl sulfate (SDS) added in the solution leads to a constructive thermophoretic force in addition to the optical gradient force, which dramatically improves the trap performance [6]. Finally, our dedicated nanoantenna design achieves a high trap stiffness of 0.6 fN/nm/mW for quantum dot trapping, together with a relatively low trapping power of 2 mW/µm² based on the photoluminescence correlation analysis of trapping events (Fig. 1c). Furthermore, the emission from the nanoantenna-trapped single quantum dot shows increased brightness, reduced blinking, shortened lifetime and a clear antibunching below 0.5 demonstrating single photon emissions (Fig. 1d) [7].

As the plasmonic nano-optical tweezer automatically locates the quantum emitter at the nanoantenna hotspot without further processing, combining nano-optical tweezers with single emitters is a promising route for quantum technologies and spectroscopy of single nano-objects.

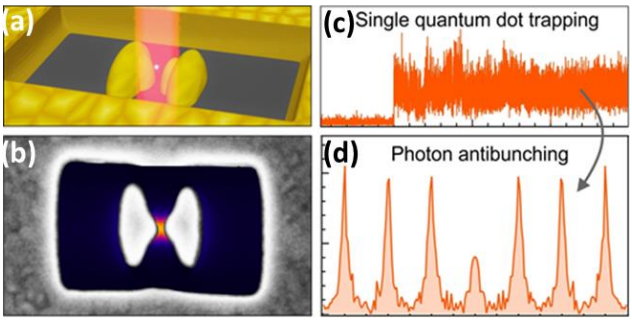

Fig. 1 (a) Sketch for plasmonic trapping of a single quantum dot. (b) SEM image of a dimmer antenna milled in gold with illustration of electric field enhancement in the gap. (c) Time trace of a trapping event for a single quantum dot. (d) Signature of single-photon emission according to the antibunching of the trapping event.

References

[1] Juan, M. L.; Righini, M.; Quidant, R. Plasmon Nano-Optical Tweezers. Nature Photonics 2011, 5 (6), 349–356.

[2] Kotnala, A.; Gordon, R. Quantification of High-Efficiency Trapping of Nanoparticles in a Double Nanohole Optical Tweezer. Nano Lett. 2014, 14 (2), 853–856.

[3] Xu, Z.; Song, W.; Crozier, K. B. Direct Particle Tracking Observation and Brownian Dynamics Simulations of a Single Nanoparticle Optically Trapped by a Plasmonic Nanoaperture. ACS Photonics 2018, 5 (7), 2850–2859.

[4] Verschueren, D. V.; Pud, S.; Shi, X.; De Angelis, L.; Kuipers, L.; Dekker, C. Label-Free Optical Detection of DNA Translocations through Plasmonic Nanopores. ACS Nano 2019, 13 (1), 61–70.

[5] Jiang, Q.; Rogez, B.; Claude, J.-B.; Baffou, G.; Wenger, J. Temperature Measurement in Plasmonic Nanoapertures Used for Optical Trapping. ACS Photonics 2019, 6 (7), 1763–1773.

[6] Jiang, Q.; Rogez, B.; Claude, J.-B.; Baffou, G.; Wenger, J. Quantifying the Role of the Surfactant and the Thermophoretic Force in Plasmonic Nano-Optical Trapping. Nano Lett. 2020, 20, 12, 8811–8817.

[7] Jiang, Q.; Roy, P.; Claude, J.-B.; Wenger, J. Single Photon Source from a Nanoantenna-Trapped Single Quantum Dot. Nano Lett. 2021, 21, 16, 7030–7036.

Invited:
Time-varying and reconfigurable driven photonics

Riccardo Sapienza
The Blackett Laboratory, Department of Physics, Imperial College London, London SW7 2BW, United Kingdom
E-mail: r.sapienza@imperial.ac.uk

Metamaterials have revolutionised the way we control light transport and generation. Yet, to date, they rely on passive architectures, only redistributing incident wave energy - for example in a metalens, or a cloak - with no power to locally absorb or produce it to enhance responses. Here I will discuss our first steps towards driven photonic systems, able to convert energy to function and perform actions.

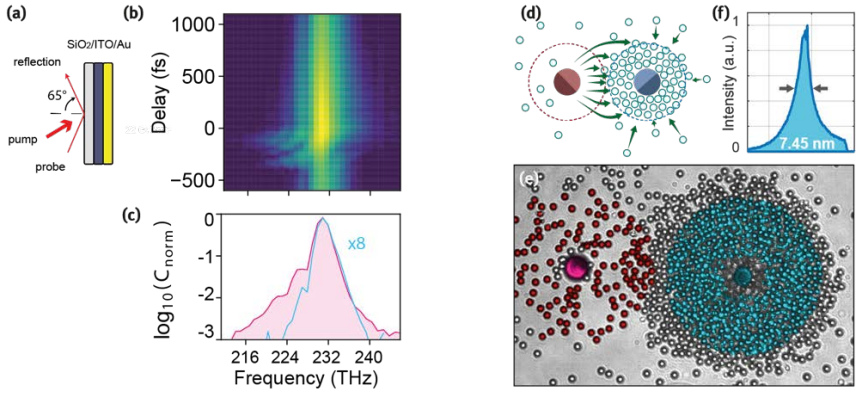

Fig. 1 A time-varying mirror composed on a ITO-Au stack (a) switches in ultrafast times, as shown in (b) as a function of the delay between pump and probe, and at high intensity (708 GW/cm^2). (c) cross-section of the reflection shown in (b), at a delay of -90 fs (pink line) as well as -500 fs delay (light blueline) where no modulation happens. (e) Switching of an active random lasing, composed of colloids as sketched in (d), when the assembly is formed (blue area in (e)) lasing action is triggered, and the spectrum narrows as shown in (f).

I will report on a switchable time-varying mirror (fig 1a), composed of an ITO-Au stack, which can be efficiently modulated in time, by a driving ultrafast laser pulse, with over a ten-fold increase in reflectivity [1]. Upon interacting with the time-varying mirror, the frequency content of a reflected pulse is extended to 31 THz with frequencies 5 bandwidths away from the original carrier frequency (fig 1b and c). This temporal response is unbounded by the pump pulse bandwidth and originates from the shortening of the response time of the mirror beyond saturation.

Moreover, I will show the self-organisation of programmable random lasers (fig1d) from the reversible out-of-equilibrium self-assembly of colloids [2]. Under external light stimuli, these dynamic random lasers are responsive and present a continuously tuneable laser threshold. They can thus reconfigure and cooperate by emulating the ever-evolving spatiotemporal relationship between structure and functionality typical of living matter.

Driven photonic systems bring novel functionalities and open the door for a new class of active functional materials towards full spatiotemporal control of light, and of fully animate lasers capable of independent motion and autonomous adaptation in response to external stimuli. This has great potential for sensing applications, non-conventional computing and novel light sources and displays.

References

[1] *Saturable time-varying mirror based on an ENZ material*, Romain Tirole, Emanuele Galiffi, Jakub Dranczewski, Taran Attavar, Benjamin Tilmann, Yao-Ting Wang, Paloma A. Huidobro, Andrea Alu˙, John B. Pendry, Stefan A. Maier, Stefano Vezzoli, and Riccardo Sapienza, arXiv: (2022).
[2] *Self-organised Lasers of Reconfigurable Colloidal Assemblies*, Manish Trivedi, Dhruv Saxena, Wai Kit Ng, Riccardo Sapienza, Giorgio Volpe, arXiv:2201.05427 (2022).

Metasurfaces for energy conversion and optical information processing

***Stefan A. Maier*[1,2,3]**

1. *School of Physics and Astronomy, Monash University, 3800 Victoria, Australia*
2. *Department of Physics, Imperial College London, London SW7 2AZ, UK*
3. *Chair in Hybrid Nanosystems, Faculty of Physics, Ludwig-Maximilians-Universität München, 80539 München, Germany*

Abstract: We present two application areas of large-area dielectric metasurfaces. Firstly, metasurfaces based on 3D direct laser writing will be discussed that operate on the orbital angular momentum degree of freedom, with applications in video holography. Secondly, nanoimprinting of GaP nanostructures facilitates photocatalytically active metasurface electrodes for applications in water splitting.

Recent advances in metasurface technologies have allowed the use of an ultrathin device to manipulate the amplitude, phase, and polarization of light, leading to a versatile platform for digitalising an optical hologram with nanoscale resolution. To increase the bandwidth of a metasurface hologram, essential for high-capacity holographic memory devices, different properties of light including polarisation, wavelength, and incident angles have been exploited for holographic multiplexing, however, the bandwidth of a metasurface hologram has remained too low for any practical use.

The orbital angular momentum (OAM) space with an unbounded set of orthogonal helical modes holds great promise to increase the bandwidth of a metasurface hologram. For achieving OAM sensitivity, a hologram needs to be designed in momentum (Fourier) space. Mathematically, a complex-amplitude hologram with complete amplitude and phase control could allow the superposition principle to continue to hold, and preserve an exact convolution of a complex-amplitude image channel and an OAM helical wavefront; hence opening the possibility of eliminating holographic multiplexing crosstalk. We present the design of a complex-amplitude metasurface hologram for OAM-multiplexing holography in momentum space, and its implementation via 3D direct laser writing [1]. Metasurface OAM holography offers a promising platform for various application areas, including optical and quantum communications, holographic displays and encryption, all-optical machine learning, biological imaging, and astronomical observations. We will furthermore present new results of the combination of laser-printed metasurfaces with optical fibres, for applications in trapping and broadband light focusing.

We further present an example for the use of dielectric metasurfaces in energy conversion. Specifically, we demonstrate how large-area nanoimprinting of GaP pillars allow the implementation of an improved electrode for photoelectrocatalysis, with enhanced absorption over the visible spectrum due to coupled anapole-type excitations. The potential and limitations of this approach for solar fuel generation will be discussed.

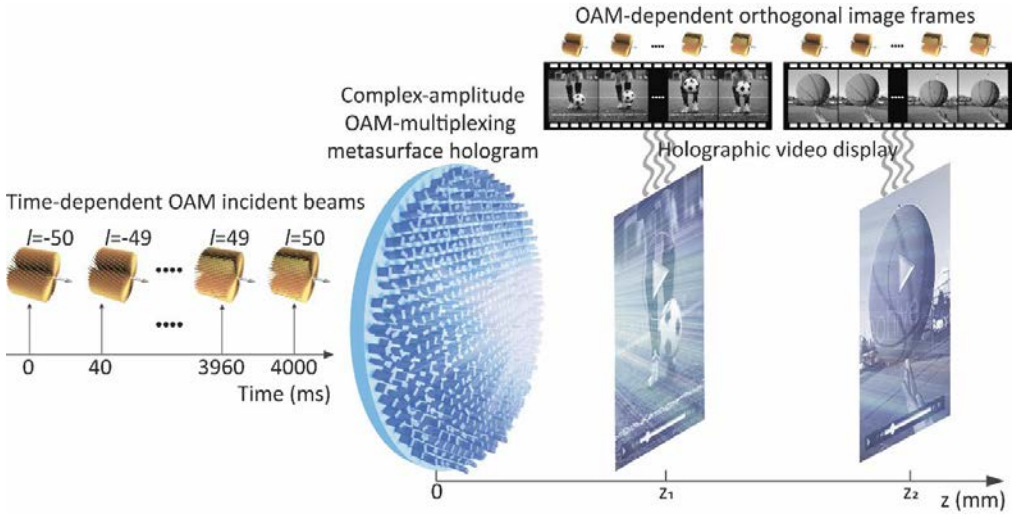

Fig. 1 Principle of ultrahigh-dimensional OAM-multiplexing holography based on a large-scale complex-amplitude metasurface hologram. Time-dependent OAM incident beams impinge on a large-scale complex-amplitude metasurface hologram to reconstruct two holographic videos consisting of a range of OAM-dependent image frames.

References

[1] H. Ren et al, "Complex-amplitude metasurface-based orbital angular momentum holography in momentum space," Nat. Nanotechnol. 15, 948-955 (2020)

[2] L. Hüttenhofer et al, “Metasurface photoelectrodes for enhanced solar fuel generation”, Adv. Energy Materials 2102877 (2021)

Wafer scale production of optical transformer-based Campanile scanning near-field probes integrated on an AFM cantilever

Adam Legacy,[1] Junze Zhou,[2] Alex Weber-Bargioni, [2] Scott Dhuey,[2] K. Munechika[1]
[1]HighRI Optics Inc, Oakland, CA, 94618
[2]The Molecular Foundry, Lawrence Berkeley National Laboratory, Berkeley, CA 94720
E-mail: km@highrioptics.com

Near-field scanning optical microscopy (NSOM) has become one of the most crucial and powerful techniques to characterize the chemical, physical, and biochemical properties of materials with nanometer-scale resolution. A key element for any NSOM system is to combine optical spectroscopy with scanning probe microscopy. An ideal NSOM probe provides a strong local electromagnetic field enhancement, efficient far-field to near- field coupling, nanoscale spatial resolution, background-free operation, and broadband photon-plasmon coupling to enable high spatial and temporal resolution. All these capabilities are combined in "campanile," which was developed and has been successfully used for multidimensional spectroscopic imaging with nanoscale resolution, observing novel optoelectronic process[1]. However, making such probes requires both the expertise and the facility, and reproducibility is a significant issue. The cost-effective production such probes is not possible with the previous fabrication efforts using Focused Ion Beam (FIB) on individual probes. There is a critical need for the development of optical tip technology to yield high-performance and reliable near-field probes and to become available to the broader user community. The realization of such probes would impact nanoscale research at the same level that atomic force microscopes did when paving the way to modern nanoscale science.

We present a wafer-scale realization of Campanile near-field scanning optical probes fabricated on an AFM platform. Figure 1 illustrates a 2D sketch and a scanning electron micrograph (SEM) image of an optical transformer on a cantilever. The optical resolution of probes depends on the nanogap, and nanogaps from 50 nm down to 6 nm were consistently and repeatedly fabricated. An index matching lens is placed on top of the Campanile to enhance the light collection efficiency from the nanogap. The figure shows the Boron Nitride flake sample and its topographical image taken by the Campanile AFM probe. Optical measurement results show a promising sign of probes' functionality with a strong polarization dependence response, which is a tell-a-tale sign of a campanile. Furthermore, we also present a used-case of an optical fiber-based imprinted "pyramid" probes, in which the researchers have successfully mapped out dark-excitonic states of WSe_2 monolayer based on the gap mode. This work paves the way for low cost and volume manufacturing of near-field probes suitable for high-resolution hyperspectral imaging.

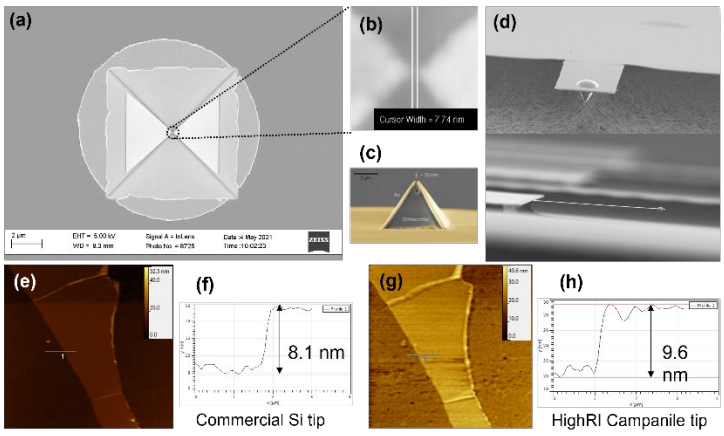

Fig. 1 (a), (b), (c), and (d) SEM images of a Campanile AFM probe. (e), (f), (g), and (h) Boron Nitride flake sample and its topography images taken by a commercial Si tip and Campanile probe.

Work at the Molecular Foundry was supported by the Office of Science, Office of Basic Energy Sciences, of the U.S. Department of Energy under Contract No. DE-AC02-05CH11231

References

[1] W. Bao, *et al.* Science 338, 1317-1321 (2012).
[2] G. Calafiore, *et al.* Scientific Reports 7, 1651 (2017).

NFO16
Real-Time In-Situ Optical Tracking of Oxygen Vacancy Migration in Memristors

Giuliana Di Martino[1,3], Angela Demetriadou[2], Weiwei Li[3], Dean Kos[1], Bonan Zhu[3], Xuejing Wang[4], Bart de Nijs[1], Haiyan Wang[4], Judith MacManus-Driscoll[3], Jeremy Baumberg[1]

1. NanoPhotonics Centre, Cavendish Laboratory, University of Cambridge, CB3 0HE, UK
2. School of Physics and Astronomy, University of Birmingham, B15 2TT, UK
3. Department of Materials Science and Metallurgy, University of Cambridge, CB3 0FS, UK
4. School of Materials Engineering, Purdue University, IN 47907-2045, USA

E-mail: gd392@cam.ac.uk

In recent years, resistive switches have been widely developed because of their low power consumption, nanosecond-scale response and logic-in-memory applications. The switching mechanism of valence change memories involves the migration, accumulation and rearrangement of oxygen vacancies within a dielectric medium to change the electrical conductivity, triggered by an external applied potential. The ability to look deep inside materials to unveil how morphological changes characterise the functioning of active devices has been vital. However, current technologies are often destructive and invasive and despite significant research efforts, a microscopic picture of how exactly the mobile species actuate device switching is still under debate [1, 2]. In-situ characterization techniques that can visualize oxygen vacancy migration in real-time and at nanoscale resolution would be hugely valuable to achieve reliable and predictable nanodevices at the wafer scale.

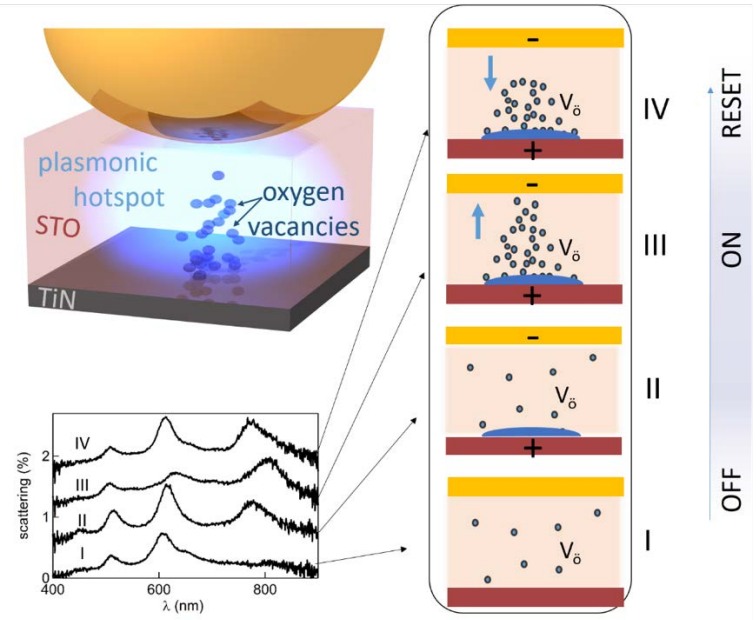

Fig. 1 | a, Valence change memristive cell (VCM) in a nanoparticle-on-mirror (NPoM) geometry, with plasmonic field tightly confined in the spacer material STO between a Au nanoparticle (NP) and TiN film **b,** giving scattering spectra for (I) pristine sample, (II) device pre-switching, (III) device switched ON and (IV) reset of device into OFF state.

We develop a novel non-destructive fully-optical technique [3] to observe in-situ and in real-time the oxygen vacancy migration within a switching material under ambient conditions, otherwise invisible to conventional electron microscopy techniques. The formation of oxygen-vacancy-induced filaments in the switching material is captured within a tightly-confined plasmonic hotspot (Fig.1a) [4]. This allows the optical measurements to be intimately linked to the electrical and material properties, hence accessing switching dynamics directly. Different optical resonances are independently sensitive to either build-up of oxygen vacancies or formation of O_2 nano-reservoirs at the interfaces (Fig. 1 b). Our spectroscopy resolves the movement of several hundred oxygen vacancies even before any electrical transport change is observed [5]. We find that oxygen vacancies build up at the material interfaces, and that O_2 bubbles of a few nm-size forming at interfaces are enough to cause long term degradation.

References

[1] Yang, J.J. et al, (2013) *Nature Nanotech*, 8, 13.
[2] Sun, W. et al, (2019) *Nat Comm*, 10, 3453.
[3] Di Martino, G. et al, (2016) *Small*, 12, 10, 1334
[4] Baumberg, J.J. et al, (2019) *Nat. Mater.* 18, 668.
[5] Di Martino, G. et al, (2020) *Nature Electronics*, 3, 687

Electrical excitation of surface plasmon polaritons with a nano-antenna tunneling junction

Delphine Pommier[1], Cheng Zhang[2], Yunhe Lai[3], Eric Le Moal[4], Christophe Sauvan[2], Jean-Jacques Greffet[2], Jianfang Wang[3], Elizabeth Boer-Duchemin[4]

1. Laboratoire de Physique des Solides, Université Paris-Saclay, Orsay, France
2. Laboratoire Charles Fabry, Institut d'Optique Graduate School, Université Paris-Saclay, Palaiseau, France
3. Department of Physics, Chinese University of Hong Kong, Hong Kong, China
4. Institut des Sciences Moléculaires d'Orsay, Université Paris-Saclay, Orsay, France

E-mail: Elizabeth.Boer-Duchemin@universite-paris-saclay.fr

Using a nano-antenna to control the emission of light is an active field [1], as is the use of a tunneling junction as a nanoscale electrical source of photons [2-4] and surface plasmon polaritons (SPPs) [5-6]. In this work, we use the tunneling junction between a nano-antenna and a thin gold film to electrically excite propagating surface plasmons and thus influence the spectrum of the excited SPPs. A novel method for completing the electrical circuit between the nano-antenna and gold film using an atomic force microscope (AFM) has also been developed in this work.

The sample consists of chemically synthesized gold nanocubes (~50-nm side length) separated from a thin (50-nm) Au film by a molecular layer (~1 nm) as shown schematically in Fig. 1a. When a conducting AFM tip is used to apply a potential difference between the nanoantenna and gold film, a tunneling current flows between the cube and substrate. The inelastic component of this current excites the available optical modes of the system. In particular, these include gap modes in the tunneling junction which locally increase the electromagnetic density of states, and an antenna mode which may be engineered to efficiently couple to the propagating SPP modes on the film. The light emitted from the excited SPPs is then detected through the transparent substrate in a leakage radiation microscopy configuration.

Figure 1b depicts the resulting spectrum in such an experiment. Two distinct peaks may be seen which, thanks to numerical modeling [7], may be identified as arising from specific gap modes or hybridized gap and antenna modes (see insets to Fig. 1b). The ability to interrogate individual nano-antennas and the theoretical comprehension of the nano-antenna junction system lead to system optimization, an enhanced excitation efficiency and the ability to control the SPP spectrum.

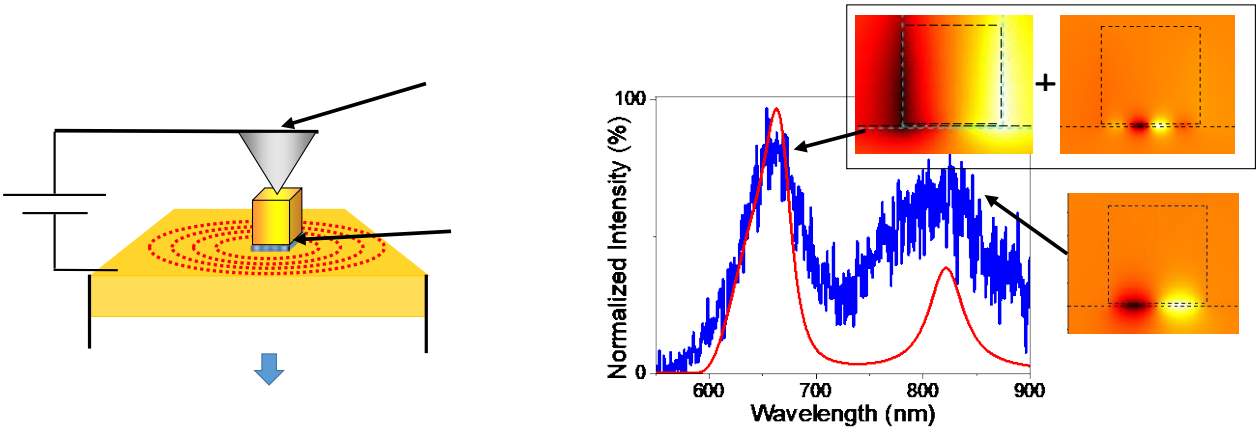

Fig. 1 a. Schematic of the experiment. A molecular layer between a nanocube antenna and a gold film acts as a tunneling junction when a voltage is applied via a conducting AFM tip. Light from the resulting SPPs is detected through the transparent substrate. b. Experimental (blue) and simulated (red) spectrum resulting from the electrical excitation of a nano-antenna junction. Insets: Maps of the *y*-component of the magnetic field in the *xz*-plane (perpendicular to the interface) show the presence of a gap mode, or of a gap + antenna mode.

References

[1] Novotny, L. and van Hulst, N. 2011. *Nat. Photonics*, 5, 83-90.
[2] Kern, J., Kullock, R., Prangsma, J., Emmerling, M., Kamp, M., Hecht, B., 2015. *Nat. Photonics*, 9, 582−586.
[3] Qian, H., Hsu, S.-W., Gurunatha, K., Riley, C. T., Zhao, J., Lu, D., Tao, A. R., Liu, Z., 2018. *Nat. Photonics*, 12, 485−488.
[4] Parzefall, M., Szabó, Á., Taniguchi, T., Watanabe, K., Luisier, M., Novotny, L., 2019. *Nat. Commun*. 10, 292.
[5] Du, W., Wang, T., Chu, H.-S., Nijhuis, C. A., 2017. *Nat. Photonics* 11, 623−627.
[6] Zhang C., Hugonin J.-P., Coutrot A.-L., Sauvan C., Marquier F., Greffet J.-J., 2019. *Nat. Commun*. 10, 4949.
[7] Zhang C., Hugonin J.-P., Greffet J.-J., Sauvan C., 2019. *ACS Photonics* 6, 2788.

Routing the Second-Harmonics Generated from a WSe2 Monolayer in a Plasmonic Nanocircuit

Pei-Yuan Wu[1], Tzu-Yu Chen[1], Wei-Qing Lee[1], Chang-Hua Liu[*, 1] and Chen-Bin Huang[*, 1]

1. Institute of Photonics Technologies, National Tsing Hua University / Hsinchu 30013, Taiwan

E-mail: (PYW)pearlwu0310@gmail.com

We experimentally demonstrate the second-harmonic signals generated in a WSe_2 monolayer can be effectively coupled into a plasmonic nanocircuit. For the first time, we show the resulting surface plasmon polaritons can be selectively routed.

The schematics of the routing design is depicted in Fig. 1(a). A three-port plasmonic circulator based on two-wire transmission-line architecture [1] is employed for the intended controllable routing of SHG. Port A is covered with a WSe_2 monolayer, upon excitation by laser beam (at fundamental frequency ω), SHGs from the WSe_2 are directly coupled into the plasmonic circulator via a designed linked antenna as surface plasmon polaritons (SPPs) at frequency 2ω. The plasmonic circulator is designed to function as a polarization splitter, based on superposition of the two modes supported by the two-wire geometry. Depending on the relative phase between the two modes, routing of SPPs is made possible to either port B or C [2]. Here, the control over the 2ω SPP routing is simply the orientation of the linearly polarized excitation laser field at frequency ω.

We first measure the polarization dependence of SHG at port A, shown in Fig. 1(b). The results are consistent to the SHG of pure TMDs and can be formulated as Eqn. (1) [3, 4]:

$$I = \cos^2 3\theta + \sin^2 3\theta \qquad (1)$$

We ensure the SPP are derived from the $WeSe_2$-SHG: in our experiment, the laser power is controlled so that there are SHG at the output port only when the laser excites port A, which is covered with WSe_2 (displayed in Fig. 1(c)). When the laser excites port B, as shown in Fig. 1(d), no SHG can be detected at either port A nor port C. With laser beam exciting port A, we vary the orientation angles of the linearly polarized excitation laser field with 10° per step. As depicted in Fig. 1(e), it is evident when the orientation angle is 10°, all SPPs are routed to port B. On the other hand in Fig. 1(f), when the laser field is changed to -20°, the SPP exit the circulator at port C. These two experimental data confirm the feasibility to achieve controllable routing of SPPs derived from SHG from $WeSe^2$. Limited by space here, we will show images for the complete angle tuning during the presentation.

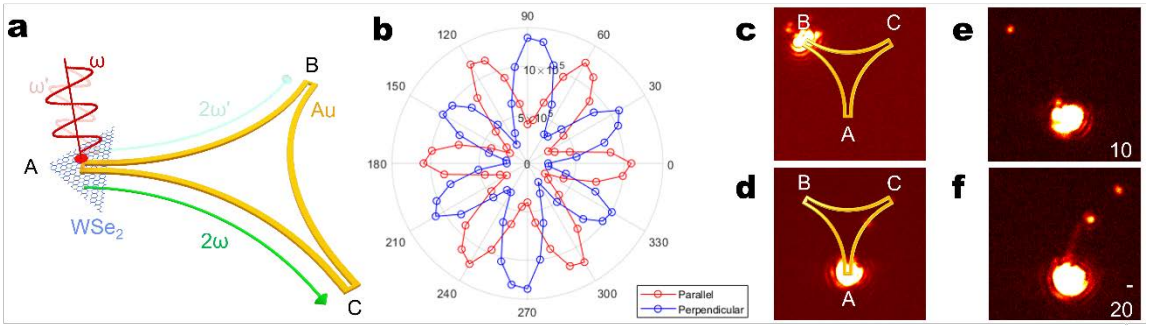

Fig. 1 (a) SHG polarization dependence of WSe2 positioned on port A. The laser power is controlled so that (b) SHG is detected only when the laser excites port A. (c) No SHG when laser excites port B. (d) 2ω SPP routed to port B when the laser field is polarized at 10 degrees. (e) 2ω SPP routed to port C when the laser field is polarized at -20 degrees.

In summary, we experimentally demonstrate the second-harmonic signals generated from a WSe2 monolayer can be effectively coupled into a plasmonic splitter to excite surface plasmon polaritons. Furthermore, we demonstrate the second-harmonic surface plasmon polaritons can be selectively routed by controlling the input fundamental frequency laser polarization. This work was supported by the Ministry of Science and Technology, Taiwan through Grants 106-2112-M-007-004-MY3 and 109-2112-M-007-031-MY3

References

[1] T.-Y. Chen et al., "Modal symmetry controlled second-harmonic generation by propagating plasmons," Nano Lett, vol. 19, no. 9, pp. 6424-6428, 2019.

[2] T.-Y. Chen, D. Tyagi, Y.-C. Chang, and C.-B. Huang, "A polarization-actuated plasmonic circulator," Nano Lett, vol. 20, no. 10, pp. 7543-7549, 2020.

[3] W.-T. Hsu et al., "Second harmonic generation from artificially stacked transition metal dichalcogenide twisted bilayers," ACS nano, vol. 8, no. 3, pp. 2951-2958, 2014.

[4] Y. Li et al., "Probing symmetry properties of few-layer MoS2 and h-BN by optical second-harmonic generation," Nano Lett, vol. 13, no. 7, pp. 3329-3333, 2013.

Exploring electrically-induced light emission mechanisms in memristive optical gap antennas

Konstantin Malchow[1], Bojun Cheng[2], Till Zellweger[2], Joerg Leuthold[2] and Alexandre Bouhelier[1]

1. Laboratoire Interdisciplinaire Carnot de Bourgogne, CNRS UMR 6303, Université Bourgogne Franche-Comté, Av. A. Savary, 21000 Dijon, France

2. ETH Zurich, Institute of Electromagnetic Fields, Zurich 8092, Switzerland

E-mail: alexandre.bouhelier@u-bourgogne.fr

Light emitted from electrically-driven optical gap antennas has been a vivid research topic over the last years [1]. The incentive is to realize fast and modulable light sources at the ultimate scale to tackle the interconnexion bottleneck in the integrated platforms [2]. The physics ruling the operation of this new generation of emitting optical antenna is quite rich, and sometimes debated. Inelastic tunneling [3], hot carrier decay [4] are highlighted as probable light emission mechanisms in devices operating in the tunneling transport regime. This simple device is also a fantastic testbed to investigate electro-optical behaviors at the interface between quantum and classical realms. Reports of Coulomb blockade [5], Fano resonances [6], charge transfer plasmons [7] and the ubiquitous role of current fluctuations [8] are discussed by the community.

Spurred by this blooming activity, we investigate the emission properties of electrically-driven optical gap antennas featuring large dielectric spacer (e.g. SiO_2), typically greater than 50 nm. We relax thereby the challenge of controlling atomic-size distances. In this gap range, photon emission cannot be understood by the processes involved in sub-nanometer junction because current transport no longer follows standard tunneling properties. Instead, such a wide-gap junction requires an electrical activation and shows a metastable resistive, akin to memristive devices [9]. We find that such volatile resistive switching is accompanied by light emission [10] as shown in the time trajectories of Fig. 1. We perform an in-depth examination of the correlation between the electron flow and light emission and carry an analysis of their temporal dynamics. Our data suggest that transport and emission are connected by metastable electroluminescent defect centers produced in the electrically-stressed dielectric gap. We further demonstrate that the emission regimes changes upon the history and resistive state of the junction. When the memristive antenna operates close to the quantum of conductance, the junction explores other radiative mechanisms. We observe a drastic change of the spectral characteristics of the photons emitted and a modification of their relationship with the transport.

Our finding suggests that a complete comprehension of the light emission mechanisms occurring in generic metal nano-gaps (electroluminescence, IET, hot electrons, etc.) needs to take into account the dynamics of electro-activation affecting the dielectric spacer.

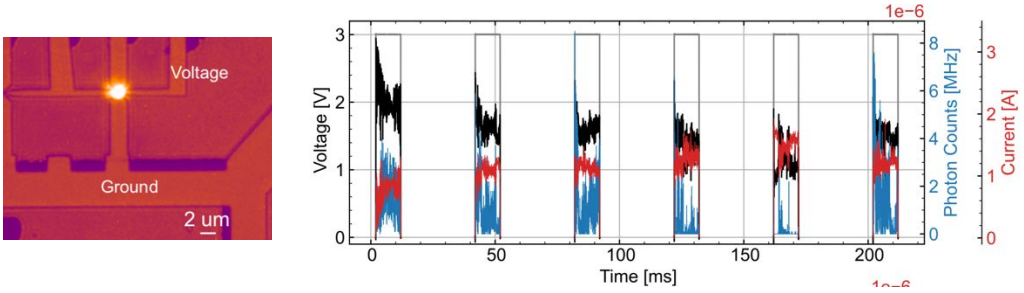

Fig. 1. Left: image showing light emission from a memristive optical gap antenna. Right: The curves show the voltage applied (grey), the voltage dropped at the device (black), the current flowing (red) and the photon count rate (blue).

References

[1] Parzefall, M., and Novotny, L. (2019). *Rep. Progr. in Phys.* 82 (11), 112401.
[2] Du W., Chu H-S, and Nijhuis C. A. (2017) *Nature Phot.* 11, 623
[3] Kullock, R. et al (2020) *Nature Com.* 11, 115
[4] Buret M. et al. (2015) *Nano Lett.*, 15, 5811; Cui. L (2020) *Nano Lett.*, 20, 6067
[5] Xiang D., Wu J., Gordon R., (2017) *Nano Lett.*, 17, 2584
[6] Vardi Y., et al (2016) *Nano Lett.*, 16, 748
[7] Paoletta A. L., Fung E.D., and Venkataraman L, (2022) *ACS Phot.* ASAP
[8] Février P, and Gabelli J., (2018) *Nature Com.* 9, 4940 ; Roslawa A., et al (2021) *Nano Lett.*, 21, 7221
[9] Cheng, B., Emboras, A., Salamin, Y. et al. (2019) *Commun Phys.* 2, 28
[10] Cheng, B., et al, (2022) *Light: Sci & Appl.* In press.

DNA origami assembled nanoantennas for manipulating single-molecule spectral emission

Maria Sanz-Paz[1], **Fangjia Zhu**[1], **Mauricio Pilo-Pais**[1], **Guillermo Acuna**[1]

1. Department of Physics, University of Fribourg, Chemin du Musée 3, Fribourg CH-1700, Switzerland
E-mail address: maria.sanz@unifr.ch

Optical antennas have been widely used for manipulating single-molecule emission properties, including intensity and decay rates, and thus for affecting lifetime, polarization, spectrum, or directivity [1,2]. Investigation of all these properties with high accuracy requires precise positioning of single molecules around the antennas, something that is still quite challenging experimentally. Here, we make use of DNA origami [3,4] as a breadboard to control the interactions between molecules and nanoantennas. By making use of a T-shaped structure, we can assemble both monomers and dimers of gold nanorods and precisely place the emitter at any desired position. We show, both numerically and experimentally, that we can affect the spectrum of a single fluorophore [5,6] in a position-dependent manner, reporting excitation of either in-phase or antiphase plasmon modes in a nanorod dimer.

References

[1] Novotny, L.; van Hulst, N. F. 2011. *Nature Photonics*, 5, 83-90
[2] Anger, P.; Bharadwaj, P.; Novotny, L. 2006. *Phys. Rev. Lett.*, 96, 113002
[3] Rothemund, P. W. K. 2006. *Nature*, 440, 297–302
[4] Pilo-Pais, M.; Acuna, G. P.; Tinnefeld, P.; Liedl, T. 2017. *MRS Bull*, 42(12), 936–942
[5] Ringler, M.; Schwemer, A.; Wunderlich, M.; Nichtl, A.; Kürzinger, K.; Klar, T. A.; Feldmann, J. 2008. *Phys. Rev. Lett.*, 100 (20), 1– 4
[6] Saemisch, L.; Liebel, M.; van Hulst, N. F. 2020. *Nano Lett.*, 20, 6, 4537–4542

Mid-infrared dielectric antennas on ENZ substrates

Francesco Rusconi[1], Pierre Felhen[2], Fernando Gonzalez-Posada[3], Laurent Cerutti[3], Giovanni Pellegrini[4], Marco Finazzi[1], Paolo Biagioni[1], Thierry Taliercio[3]

[1]Dipartimento di Fisica, Politecnico di Milano, Milano, 20133 Italy
[2]NSE3 (CNRS UMR3208) Institut franco-allemand Saint-Louis, France
[3]IES, Univ Montpellier, UMR CNRS 5214, Montpellier, France
[4]Dipartimento di Fisica, Università di Pavia, Pavia, Italy
E-mail: francesco.rusconi@polimi.it

Nanoantennas play a major role in light manipulation at the nanoscale. This is achieved by exploiting their resonances, which present highly confined and enhanced local fields [1]. The traditional materials of choice for nanoantennas are noble metals, however, there are intrinsic limitations associated to their use. In fact, plasmonic resonances suffer from ohmic losses, affecting the quality factor and the lifespan of the antenna itself. Moreover, magnetic resonances supported by metallic plasmonic antennas are weak, which is detrimental for specific applications such as those requiring enhanced optical chirality [2, 3].

In the last years, dielectric nanoantennas have been proposed as an alternative to plasmonics. While there are many demonstrations for dielectric nanoantennas working in the visible and near-infrared spectral range [3-6], their extension to the mid infrared (MIR) is not yet fully established. In particular, the epitaxial growth of crystalline semiconductor materials, which are the preferred choices for high-quality dielectric antennas working in the MIR, typically relies on a similar semiconductor substrate, with a refractive index close to the one of the antenna. This environment configuration hinders the establishment of strong resonances for dielectric antennas in the MIR.

In this work, as a solution to this problem, we employ a highly-doped InAs layer as the substrate [7]. By properly varying the doping of the InAs layer we obtain a material showing a zero crossing of the real part of the permittivity, the so-called epsilon-near-zero (ENZ) condition [8], that can be tuned over a broad wavelength range in the MIR. We fabricate an array of dielectric nanoantennas on top of the ENZ substrate exploiting an undoped InAs layer by standard e-beam lithography (Figure 1a). By spectrally overlapping the localized and lattice resonance frequencies of the antenna array with the ENZ frequency of the substrate, we observe a sharp resonance (figure 1b). Numerical electromagnetic simulations also demonstrate that the associated field enhancements are expected to reach values similar to the ideal situation of the same antennas in vacuum. The demonstration of a dielectric platform working in the MIR opens new possibilities in surface-enhanced spectroscopy, biosensing, and chiroptical analysis.

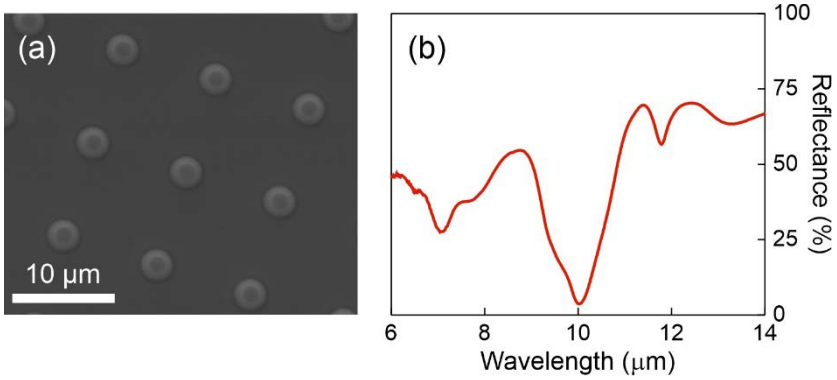

Fig. 1 Scanning electron microscope top view of the InAs nanoantennas (panel a) and the spectral response of the array (panel b). The reflectance spectrum is taken by using a Fourier-transform interferometer coupled with an optical microscope.

References

[1] Biagioni, P.; Huang, J-S.; Hecht, B. 2012. *Rep. Prog. Phys.* 75, 024402.
[2] García-Etxarri, A. ; Dionne, J. 2013. *Phys. Rev. B.* 87, 235409.
[3] García-Guirado, J.; Svedendahl, M.; Puigdollers, J.; Quidant, R. 2020. *Nano Lett.* 20, 1, 585–591.
[4] Albella, P.; de la Osa, R.A.; Moreno, F.; Maier, S.A.; 2014. *Acs Photonics.* 1, 6, 524–529.
[5] Kuznetsov, A.I.; Miroshnichenko, A.E.; Brongersma, M.L.; Kivshar, Y.S.; Luk'yanchuk, B.; 2016. *Science.* 354, 6314.
[6] Zilli, A.; Rocco, D.; Finazzi, M.; Di Francescantonio, A.; Duò, L.; Gigli, C.; Marino, G.; Leo, G.; De Angelis, C.; Celebrano, M.; 2021. *ACS Photonics.* 8, 4, 1175–1182.
[7] Bahro, B.F.; Gonzales-Posada, F.; Milla-Rodrigo, M-J.; Bomers, M.; Cerutti, L.; Taliercio, T.; 2016. *Opt. Express.* 24, 16175-16190.
[8] Kim, J.; Dutta, A.; Naik, G.V.; Giles, A.J.; Bezares, F J.; Ellis, C.T.; Tischler, J.G.; Mahmoud, A.M.; Caglayan, H.; Glembocki, O.J.; Kildishev, A.V.; Caldwell, J.D.; Boltasseva, A.; Engheta, N. 2016. *Optica*. 3, 339-346.

Mode-selective imaging and control of nano-plasmonic near-fields

Hugo Lourenço-Martins[1,2,3], **Murat Sivis**[1,2], **Andre Geese**[1], **Tyler R. Harvey**[1], **Thomas Danz**[1,2], **Radwan M. Sarhan**[4], **Matias Bargheer**[4], **Armin Feist**[1,2], **Claus Ropers**[1,2]

1. Max Planck Institute for Multidisciplinary Sciences, 37077 Göttingen, Germany
2. IV. Physical Institute, University of Göttingen, 37077 Göttingen, Germany
3. CEMES-CNRS, Université de Toulouse, CNRS, Toulouse, France
4. Institut für Physik und Astronomie, Universität Potsdam, 14476 Potsdam, Germany
e-mail: hugo.lourenco-martins@cemes.fr

Electron energy-loss spectroscopy (EELS) in a transmission electron microscope (TEM) is a powerful technique to probe optical and electronic excitations with a sub-nanometer spatial resolution [1, 2]. However, probing spontaneous losses, this technique does not provide time-domain access to ultrafast processes and is restricted in its spectral resolution even for the most advanced electron sources available (10-100 meV).
Here, recent developments in the field of ultrafast transmission electron microscopy (UTEM) promise to overcome these limitations by probing laser-excited optical modes with femtosecond electron pulses. Specifically, in a stroboscopic laser-pump/electron probe scheme, an optically excited sample is measured with photo-emitted ultrashort electron wave-packets [3] and scanning their relative time delay gives access to the involved ultrafast dynamics. Such an instrument thus combines the spatial resolution of a conventional TEM (nm) with the unrivaled spectral and temporal resolutions provided by ultrafast lasers (resp. sub-meV and hundreds of femtoseconds), and therefore offers unique capabilities to probe optical fields at the nanoscale.

In this talk, I will demonstrate how this technique – usually referred to as photon-induced near-field electron microscopy (PINEM) – can be used to analyze the modal structure of the optical response of individual plasmonic nano-resonators (gold and silver nano-triangles) directly at the nanoscale. We will present our boundary element method (BEM)-based data analysis which enable us to extract from optical near-field maps, the magnitude and relative phase of each plasmonic modes excited by a femtosecond pump laser, as illustrated on figure 1. Thanks to this method, we will analyze the influence of the laser polarization, wavelength and incidence angle on the population of each modes. Particularly, we will show that the total optical near-field excited by the laser, result from the interference pattern of a large number of plasmonic modes which can be controlled by tuning the laser properties. Finally, we will theoretically and experimentally demonstrate that the plasmonic optical near-field can be coherently manipulated by pumping the system with two phase-locked optical pulses of different wavelength, which enables to create a complex beating pattern between two different plasmonic modes in the same single nano-resonator.

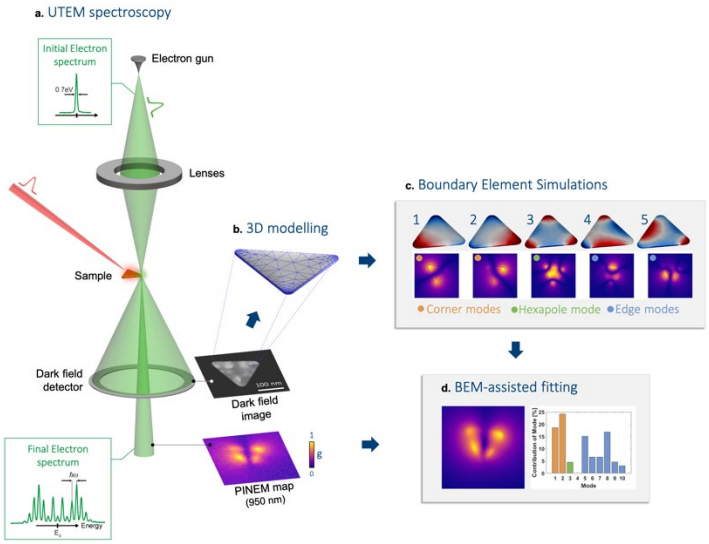

Fig. 1 Illustration of the BEM mode analysis approach developed in this work. a. A nanometer resolved map of the optical near field associated to the plasmons pumped by a femtosecond laser is recorded by EELS. b. The associated TEM image is processed to extract the 3D geometry of the nanostructure. c. The model is used to compute the plasmonic eigenmode of the structures. d. Based on a L1-L2 optimization procedure, the magnitude and relative phase of each modes is reconstructed from the near-field map.

References

[1] J. Nelayah et al., " Mapping surface plasmons on a single metallic nanoparticle", *Nat. Phys. 3, 348–353 (2007)*
[2] H. Lourenço-Martins et al., " Self-hybridization within non-Hermitian localized plasmonic systems", *Nat. Phys. 14, 360–364 (2018)*
[3] A.Feist et al., " Quantum xscoherent optical phase modulation in an ultrafast transmission electron microscope" *Nature 521, 200–203 (2015)*

Molecules on Whispering Gallery Modes: Single Molecule Sensing and Beyond

Frank Vollmer[1]

[1]Department of Physics & Astronomy, University of Exeter

E-mail: F.Vollmer@exeter.ac.uk

Single molecule sensing based on the hybridization of WGM optical microcavities and localized surface plasmon resonances in metal nanoparticles has emerged as one of the most sensitive biodetection technology. I will give an ample survey of the physical and biological sensing mechanisms of these optoplasmonic sensors and their applications in fundamental and applied studies of optical and molecular interactions.

Viewing interfacial chemistry through a graphene window

Hans A. Bechtel[1], **Jonathan M. Larson**[2], **Xin He**[2], **Xiao Zhao**[3,4], **Dong Li**[5], **Yi-Hsien Lu**[3], **Behzad Rad**[5], **Chunsheng Yan**[5], **Paul D. Ashby**[5], **Stephanie Gilbert Corder**[1], **Miquel Salmeron**[3,4], **Robert Kostecki**[2]

1. Advanced Light Source, Lawrence Berkeley National Laboratory, Berkeley, CA 94720 USA
2. Energy Storage & Distributed Resources Division, Lawrence Berkeley National Laboratory, Berkeley, California, 94720, USA
3. Materials Sciences Division, Lawrence Berkeley National Laboratory, Berkeley, California, 94720, USA
4. Department of Materials Science and Engineering, University of California at Berkeley, Berkeley, California 94720, USA
5. Molecular Foundry, Lawrence Berkeley National Laboratory, Berkeley, California, 94720, USA

E-mail: habechtel@lbl.gov

The functionality of natural and engineered systems is often determined by the chemical interactions that occur at the interface of two or more materials. Characterizing such interfaces in their native environment, however, is extremely challenging because the interfacial region is often buried by the bulk materials and the interfacial chemistry can span multiple spatial scales. Here, we exploit the nanoscale spatial resolution, chemical selectivity, and surface sensitivity of near-field infrared nanospectroscopy (nano-FTIR) to explore the dynamics of protein self-assembly in aqueous solutions and to characterize the solid-electrolyte interphase (SEI) layer in a model solid-state electrochemical cell [1]. In both applications, we use graphene as an ultra-thin IR transparent "coverslip" that serves as an impermeable barrier to protect the interfacial region from contamination or oxidation and allow ambient conditions on the probe side while enabling direct access to the interfacial region between the liquid or solid-state solutions, respectively [2]. *In-vitro* measurements using the liquid cell show the formation of S-layer protein lattices by monitoring the response of Amide-I and Amide-II absorption bands to environment variables, including ionic strength and solvent [3]. The non-linear growth of these bands mirrors the increase in the percentage of the ordered protein domains obtained from AFM images but with inhomogeneous spatial distributions not previously seen. *In-situ* measurements of the electrochemical cell reveal that intrinsic molecular, structural, and chemical heterogeneities in the solid polymer electrolyte lead to nonuniform Li plating and formation of a mosaic-like solid electrolyte interphase of similar length scales [4]. These studies provide a unique insight into the mechanisms of interfacial chemistry and an experimental diagnostic means to aid in the development of methods to control local nanoscale variations in biological and electrochemical systems.

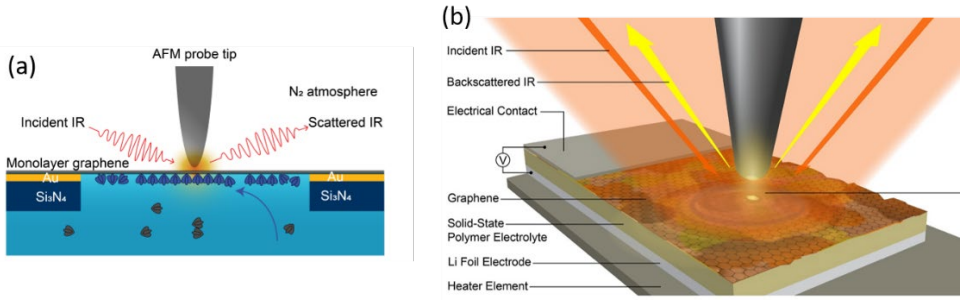

Fig. 1 Schematics of (a) the aqueous cell for *in vitro* protein self-assembly measurements and (b) the model solid-state battery cell for *in situ* electrochemical measurements of the graphene/lithium/polymer electrolyte interface.

References

[1] Bechtel, H. A.; Johnson, S. C.; Khatib, O.; Muller, E. A.; Raschke, M. B. 2020. *Surface Science Reports*, 75, 100493.
[2] Lu, Y.-H.; Larson, J. M.; Baskin, A.; Zhao, X.; Ashby, P.D.; Prendergast, D.; Bechtel, H. A.; Kostecki, R.; Salmeron, M. B. 2019. *Nano Lett.*, 19, 5388-5393.
[3] Zhao, X.; Li, D.; Lu, Y.-H.; Rad, B.; Yan, C.; Bechtel, H. A.; Ashby, P.; Salmeron, M. B. 2022, *in press*.
[4] He, X.; Larson, J. M.; Bechtel, H. A.; Kostecki, R. 2022, *in press*.

Viral Diagnosis using Nanoscale Vibrational Spectroscopy

Volker Deckert[1,2]

1. Leibniz Institute of Photonic Technology, Albert-Einstein-Str. 11, 07745 Jena, Germany
2. Institute of Physical Chemistry and Abbe Center of Photonics, Helmholtzweg 4, 07743 Jena, Germany
E-mail: Volker.deckert@uni-jena.de

Antibody and PCA tests are standard for the diagnosis of viral infections, but specific (sensitive) antibodies and the required DNA sequence are not readily available, especially in the early stages of infections via novel variants. Therefore, we investigated the possibility of using label-free methods for virus identification. Direct spectroscopic diagnosis, which has already been developed for bacterial infections, is generally difficult because the dimensions of individual viruses are well below the optical diffraction limit and purification and pathogen enrichment techniques for standard spectroscopies are very elaborate and expensive.

We use a scanning probe approach to look for individual "virus-like" particles in cultured and actual samples. In this way, we can already pre-select potential viral candidates based on size and shape and distinguish them from cell debris and, in our case, crystallized inactivation chemicals. The method was tested by stepwise correlation of AFM topography of known virus strands (SARS-CoV-2) with fluorescence experiments. In a first step, RNA-stained virus particle fluorescence images are correlated with AFM topography experiments and show excellent agreement ensuring that indeed viral particles have been identified. In a 2nd step, antibody staining (now at the virus surface) was applied to the immobilized particles. Again, the images correlate with the topography images and show that pre-selection is possible by topography alone. Force-distance experiments were performed on the sample particles to obtain nano-mechanical parameters (Youngs modulus, adhesion). This not only allows to distinguish the virus particles from other particles of similar size, but also indicates variations in the virus particles and can be used to further subdivide the viruses (infectious, non-infectious). Last but not least, the virus particles were examined using tip-enhanced Raman spectroscopy. A major challenge here is the extreme local resolution of TERS compared to the specimen size, as for a diagnosis one is less interested in specific local composition of a virus surface, but rather the “averaged” structural composition. For this purpose, we compare standard TERS maps with TERS spectra acquired during a topography scan. The latter simply averages continuously the Raman signal over the scan area. We can show that while the localized spectra show a quite strong changes from one position to the next, the ones acquired “while scanning” not only show less features but are also much more reproducible from one TERS experiment to the next. This not only confirms that this can be used for a structural diagnosis, but it further is also in well agreement with the now generally understood extreme lateral resolution of TERS.

References

[1] V. Deckert *et al.*, Laser spectroscopic technique for direct identification of a single virus I: FASTER CARS. *Proceedings of the National Academy of Sciences*. **117**, 27820–27824 (2020).
[2] K. Olschewski *et al.*, A manual and an automatic TERS based virus discrimination. *Nanoscale*. **7**, 4545–4552 (2015).
[3] D. Cialla *et al.*, Raman to the limit: tip-enhanced Raman spectroscopic investigations of a single tobacco mosaic virus. *J Raman Spectrosc*. **40**, 240–243 (2009).

IR nanoscopy of flat-membrane-covered living cells in water

Fritz Keilmann[1], **Korbinian Kaltenecker**[2], **Thorsten Gölz**[1], **Enrico Bau**[1]

1. Fakultät für Physik, Nano Institute Munich & Center for NanoScience (CeNS), LMU, Königinstr. 10, 80539 Munich, Germany
2. Attocube Systems AG, Eglfinger Weg 2, 85540 Haar, Germany
E-mail: fritz.keilmann@lmu.de

We report scattering-type near-field microscopy through an ultrathin membrane cover (Fig. 1a) of water-suspended precision microspheres and even of living cells in nutrient broth [1]. The employed 10-nm thick SiN membrane is transparent from visible to 10 µm wavelengths, commercially available (norcada.com), and perfectly flat. Importantly, it is robust enough to withstand the tip's tapping on its upper surface, as well as the forces exerted to its underside both by its contact to liquid and by particle adhesion, even at 250 µm free spanning.

Adhesion of test particles and living cells deforms the membrane measurably such that the AFM records, in addition to the optical amplitude and phase images, purely mechanical images of both topography and tapping phase. This provides a novel contrast mechanism in scanning-probe microscopy and certainly adds valuable correlative information to near-field optical images.

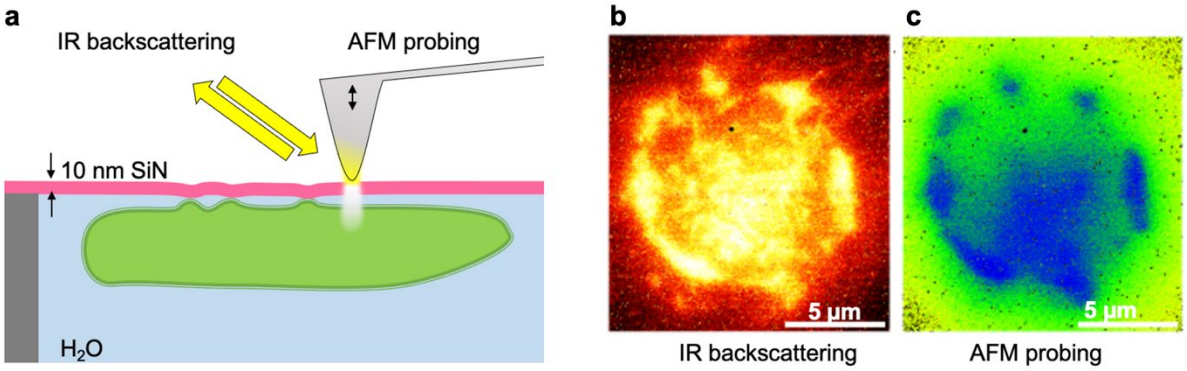

Fig. 1 Sketch (**a**) and results (**b,c**) of in-vivo imaging a lung cancer cell of type A549, prepared by simply drop-casting a liquid culture onto the 10-nm thin SiN membrane where cells adhere. The infrared backscattering image (**b**) maps the cell's morphology in <150-nm detail, whereas the simultaneous AFM probing (**c**) clearly exhibits a correlated mechanical phase contrast image, interpreted as the cell's adhesion footprint. The setup allows following the cell's growth dynamics uninterrupted over days.

The tip-confined near-field (visualized as white cloud) penetrates the membrane without loss and maps a particle's or living cell's local optical response, in Fig. 1b spectrally averaged from 6 to 9 µm. When operated with broad-band mid-infrared illumination and interferometric detection [2] the recorded (nano-FTIR) spectrum contains characteristic molecular vibration bands which enable quantifying the chemical composition, for example, a living cell's local abundances simultaneously of protein, lipid, DNA and water.

For calibrating the near-field interaction, nano-FTIR imaging and spectroscopy can conveniently probe well-defined objects such as a large PMMA sphere adhering to the membrane. A radial scan then accurately measures, as the PMMA surface submerges, the decay of PMMA spectral peaks and the concomitant rise of water peaks. We find excellent agreement with calculations based on the multilayer theory of near-field interaction in the finite-dipole approximation [3]. As an important result we find that it is at a typical submersion depth of 70 ± 10 nm that near-field probing through the membrane decreases to one half of its value at 0 nm (contact).

Our novel tool of nano-imaging that keeps wet samples stable and returns structure, dynamics and chemical composition should benefit the nanoscale analysis of any aqueous system, from physics to medicine. It should advance our understanding of processes such as the corrosion of steel in concrete or the spatio-temporal course of a chemical reaction in close proximity to a nanosized catalyst. Potential applications for live cell nano-imaging could include cell migration and cell differentiation. Possibly one can observe aggregation processes of proteins *in situ*, expected to play a key role in Alzheimer's and other neurodegenerative diseases.

References

[1] K.J. Kaltenecker KJ, Gölz T, Bau E, Keilmann F. 2021. Infrared-spectroscopic, dynamic near-field microscopy of living cells and nanoparticles in water. *Scientific Reports* 11:2860, doi.org/10.1038/s41598-021-01425-w.
[2] Huth F, Govyadinov A, Amarie S, Nuansing W, Keilmann F, Hillenbrand R. 2012. Nano-FTIR absorption spectroscopy of molecular fingerprints at 20nm spatial resolution. *NanoLett.*12, 3973–3978.
[3] Hauer B, Engelhardt AP, Taubner T. 2012. Quasi-analytical model for scattering infrared near-field microscopy on layered systems. *Opt. Express* 20, 13173–13188.

Vibrational exciton nanoscopy: a molecular ruler to image structure, coupling, and disorder on their elementary scales

Thomas P. Gray[1], **Eric A. Muller**[2], **Jun Nishida**[1], **Richard L. Puro, and Markus B. Raschke**[1]

1. Department of Physics and JILA, University of Colorado Boulder, Boulder, CO 80309, USA
2. Department of Chemistry, Colgate University, Hamilton, NY 13346, USA
Email : Thomas.P.Gray@colorado.edu, Richard.Puro@colorado.edu, Markus.Raschke@colorado.edu

Many properties of biomolecular, photophysical, and molecular energy materials emerge from intermolecular interactions. However, associated defects and disorder give rise to confinement and many-body localization of the associated wavefunction, disturbing the performance of the material. Most conventional microscopy techniques lack sensitivity to the low-energy scales of intermolecular interactions, leaving a missing link between material structure and heterogeneity in the electronic or photonic response.

Here, we address this outstanding problem using infrared scattering scanning near-field optical microscopy (IR *s*-SNOM) to resolve *intermolecular coupling* and its disturbance through structural disorder. Specifically, we measure transition dipole (μ) coupling between molecules in the form of *vibrational excitons* (Fig.1 D). Vibrational excitons manifest themselves as vibrational peak shifts correlated with vibrational wavefunction delocalization length, and thus allow imaging *correlation length* of molecular order associated with molecular order, crystallinity, or domain size.

Following our previous work on the study of defects in growth of competing amorphous and crystalline phases in porphyrin electronic nano-materials [1], here we extend vibrational exciton nanoscopy to imaging intra- and intermolecular vibrational coupling in polymers [2], and molecular monolayers [3]. In poly(tetrafluoroethylene) (PTFE), we observe exceptionally large spatio-spectral heterogeneities with C-F vibrational energy shifts ranging from sub-cm^{-1} to ≳25 cm^{-1} reflecting a high degree of local crystallinity interspersed with amorphous disorder (Fig.1 B,C). Combining vibrational exciton nanoimaging in variable-temperature IR *s*-SNOM with four-dimensional scanning transmission electron microscopy (4D-STEM), and vibrational exciton modeling based on density functional theory (DFT), we were able to link local microscopic molecular interactions to macroscopic three-dimensional order [2].

Further, domain formation determines carrier transport or wettability of self-assembled monolayers (SAMs) through collective effects. In the model system of a 4-nitrothiophenol (4-NTP) on gold, we resolve in spatio-spectral nano-imaging heterogeneity in intermolecular coupling with sub-monolayer sensitivity. From modeling the underlying 2D coupling Hamiltonian, we infer domain sizes and their distribution from 3 to 12 nm across (Fig.1 E-G) [3].

In summary, these examples show the general applicability of vibrational exciton nano-imaging to provide the molecular level insight into the functional interactions that define the properties of a wide range of molecular materials.

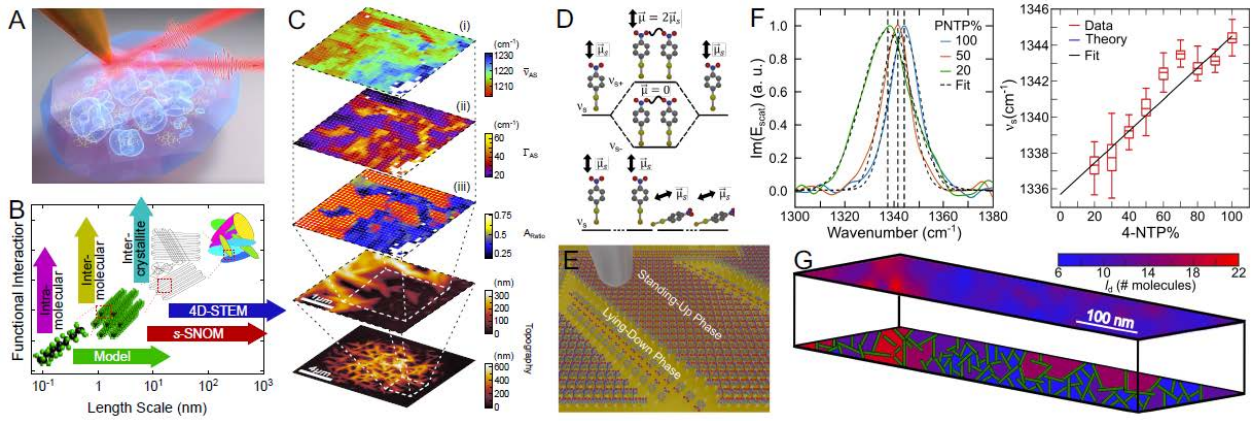

Fig. 1 (A) Infrared nano-imaging of intermolecular coupling-induced vibrational wavefunction delocalization. (B) Length scales of intra- and intermolecular interaction. (C) Spatio-spectral nano-imaging of PTFE resolving crystalline and amorphous domains from coupling induced vibrational peak shifts. (D) Interaction Hamiltonian describing underlying mode splitting and spectral shift depending on molecular orientation and order. (E) Vibrational exciton nano-imaging resolving domain formation in self-assembled monolayer, deriving from vibrational peak shift and dilution experiments (F) the few-nanometer domain size distribution.

References

[1] E. A. Muller, T. P. Gray, Z. Zhou, X. Cheng, O. Khatib, H. A. Bechtel, and M. B. Raschke, *"Vibrational exciton nanoimaging of phases and domains in porphyrin nanocrystals"*, PNAS **117**, 7030 (2020).
[2] S. Dönges, P. R. Cline, S. Zeltmann, J. Nishida, B. Metzger, A. Minor, J. Eaves, and M. B. Raschke, *"Multidimensional nano-imaging of structure, coupling, and disorder in molecular materials"*, Nano Lett. **21**, 6463 (2021).
[3] T. P. Gray, J. Nishida, S. C. Johnson, and M. B. Raschke, *"2D Vibrational exciton nanoimaging of domain formation in self-assembled monolayers"*, Nano Lett. **21**, 5754 (2021).

Modelling photothermal induced resonance microscopy: the role of interface thermal resistances

Paolo Biagioni[1], **Francesco Rusconi**[1], **Marco Finazzi**[1], **John M. Stormonth-Darling**[2], **Gordon Mills**[2], **Michela Badioli**[3], **Leonetta Baldassarre**[3], **Michele Ortolani**[3,4], **Valeria Giliberti**[4].

1. Dipartimento di Fisica, Politecnico di Milano, Piazza Leonardo da Vinci 32, I-20133 Milano, Italy
2. Kelvin Nanotechnology Ltd, Rankine Building, Oakfield Ave, Glasgow, G12 8LT, UK
3. Department of Physics, Sapienza University of Rome, Piazzale Aldo Moro 2, I-00185 Roma, Italy
4. Istituto Italiano di Tecnologia, Center for Life Nano- & Neuro-Science, Viale Regina Elena 291, I-00161 Roma, Italy

E-mail: paolo.biagioni@polimi.it

Photothermal induced resonance (PTIR) microscopy is an experimental technique that combines the resonant absorption of infrared (IR) light with the measurement of the thermal expansion of the sample by atomic force microscopy (AFM) [1-5]. With this technique, it is possible to determine the chemical and conformational properties of the sample (relying on IR absorption spectroscopy) at the nanoscale (thanks to the lateral resolution provided by AFM). However, since the development of PTIR microscopy is still relatively new, there is yet no common established procedure in the modelling of the experimental data.

In this work we consider two experimental datasets, obtained with two different AFM tips (a standard gold-coated silicon tip and a triangular silicon nitride tip with a resonant palladium antenna at its end), investigating a PMMA whisker with varying thickness (10-400 nm) [6]. Thanks to this consistent set of experimental data, we find ourselves in the position to assess the validity of combined optical and thermal simulations for the analysis of the PTIR experiment (Fig. 1a), especially demonstrating the crucial role played by interface thermal resistances in determining the dependence of the signal on the sample thickness (Fig. 1b,c). Moreover, we highlight a further contribution to the thickness dependence associated with the field confinement properties of the AFM tip, providing evidence that the concentration of electromagnetic energy by the resonant antenna tip increases the surface sensitivity of the technique. These results represent a step ahead in the establishment of a common ground for the quantitative analysis of PTIR data.

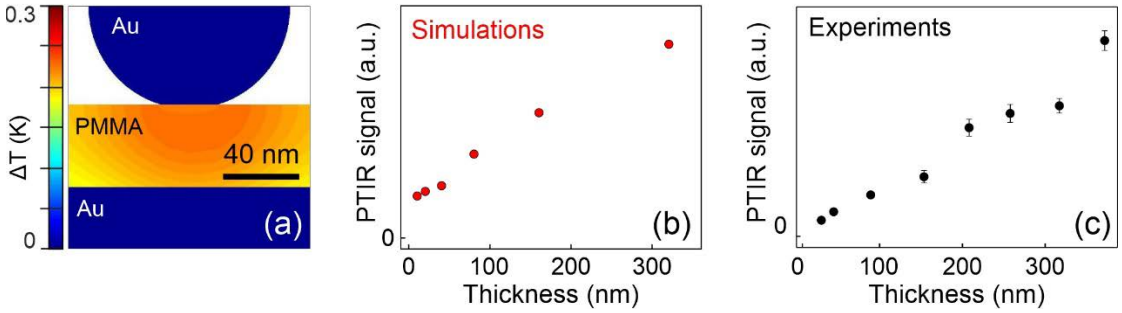

Fig. 1 Representative finite-element thermal simulations of the sample response after resonant IR illumination for a standard Au-coated AFM tip (panel a) and the calculated PTIR signal as a function of the thickness of the PMMA layer (panel b). The numerical results confirm a characteristic linear dependence also observed in the experiments (panel c), which cannot be reproduced unless interface thermal resistances are considered in the simulations.

References

[1] Dazzi, A.; Glotin, F.; Carminati, R. 2010. *J. Appl. Phys.* 107, 124519.
[2] Lu, F.; Jin, M.; Belkin, M. A. 2014. *Nature Photonics* 8, 307-312.
[3] Chae, J.; An, S.; Ramer, G.; Stavila, V.; Holland, G.; Yoon, Y.; Talin, A. A.; Allendorf, M.; Aksyuk, V. A. ; Centrone, A. 2017. *Nano Lett.* 17, 5587-5594.
[4] O'Callahan, B. T.; Yan, J.; Menges, F.; Muller, E. A.; Raschke, M. B. 2018. *Nano Lett.* 18, 5499-5505.
[5] Giliberti, V.; Polito, R.; Ritter, E.; Broser, M.; Hegemann, P.; Puskar, L.; Schade, U.; Zanetti-Polzi, L.; Daidone, I.; Corni, S.; Rusconi, F.; Biagioni, P.; Baldassarre, L.; Ortolani, M. 2019. *Nano Lett.* 19, 3104-3114.
[6] Rusconi, F.; Finazzi, M.; Stormonth-Darling, J. M.; Mills, G.; Badioli, M.; Baldassarre, L.; Ortolani, M.; Biagioni, P.; Giliberti, V. 2021. arXiv:2111.07303.

Synchrotron Infrared Nanospectroscopic Measurements of Biaxial Anisotropy: Hyperbolic Phonon Polaritons and a Novel Method for Determining the In-Plane Permittivity

Stephanie N. Gilbert Corder[1], Hans A. Bechtel[1], Shangjie Yu[2], Jonathan Fan[2], Ziheng Yao[3], Mengkun Liu[3]

1. Advanced Light Source, Laurence Berkeley National Laboratory, 1 Cyclotron Rd, Berkeley, CA 94720-8226
2. Department of Electrical Engineering, Stanford University, Stanford, CA 94305
3. Department of Physics and Astronomy, Stony Brook University, Stony Brook, NY 11790

E-mail: sgilbertcorder@lbl.gov

Synchrotron infrared nanospectroscopy (SINS) combines the broad bandwidth and brightness of synchrotron infrared radiation with scanning near-field optical microscopy (s-SNOM), enabling direct probing of elementary excitations of functional materials spanning the mid- and far-infrared with < 20 nm spatial resolution. The Advanced Light Source (ALS) at Lawrence Berkeley National Laboratory operates two infrared beamlines (Beamlines 2.4 and 5.4) with SINS instruments that are freely available to users with an approved scientific proposal. Here, we highlight the capabilities of the ALS infrared beamlines by investigating the propagation of anisotropic hyperbolic phonon polaritons within crystalline microstructures and by measuring the in-plane phonon responses of anisotropic crystalline materials with an antenna-assisted geometry.

We present recent results on ultrahigh-quality biaxial phonon polaritons in van der Waals nanoribbons. These bottom-up-synthesized α-MoO_3 nanoribbons form low-loss hyperbolic Fabry-Pérot resonators, demonstrating modes up to the 10th order. These resonances can be tailored by selecting nanoribbons with different thicknesses and widths. Using a microplate structure, we are able to map the hyperbolic response over four Reststrahlen bands in the mid- and far-infrared spectral range. The mode confinement and low losses demonstrated by the materials make it an ideal platform for studying fundamental light-matter interactions and may enable research advances in infrared photonic systems. [1]

Additionally, a method of obtaining the in-plane dielectric response with near-field spectroscopy is discussed. By depositing a gold disk antenna on the material surface, the typical limitations of measuring in-plane anisotropies are circumvented: the antenna couples the interaction of the disk and substrate to the out-of-plane localized electric field. We are therefore able to measure the LO phonon modes along the *b*- and *c*-axes of (100) sapphire with a resolution of λ/10. The method is further used to identify the orientation of the optical axis of $LiNbO_3$. This scheme could be employed to determine the in-plane anisotropy of a variety of material systems; a significant step towards obtaining complete nanoscale dielectric tensors.[2]

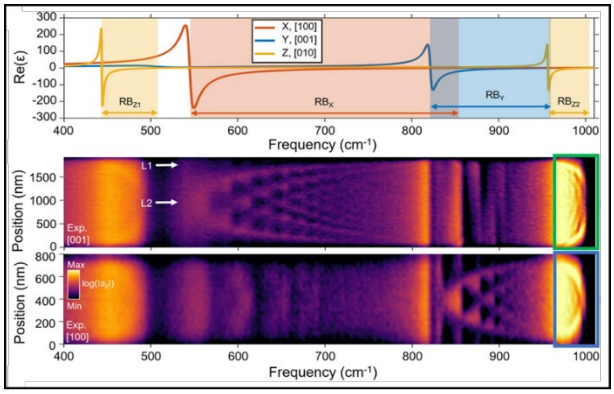

Fig. 1 Nanospectroscopy of α–MoO_3 nanoribbon on ultra-smooth gold. The real part of the permittivity (top) is shown with four Reststrahlen bands. The high-quality phonon-polariton modes along the [001] and [100] crystallographic directions are shown in the middle and lower panels [1].

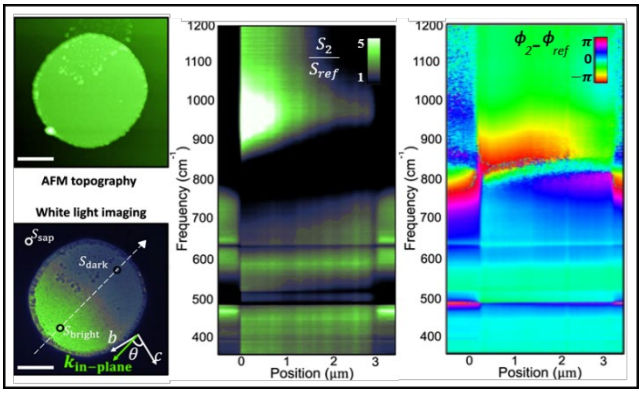

Fig. 2 Nanospectroscopy of gold disk antennas on (100) sapphire. AFM topography and white light near-field imaging show a gold antenna disk and the direction of measurement from bright region to dark. The near-field amplitude (center) and phase (right) are shown as a function of position across the antenna [2].

References

[1] Yu, S.-J., Jiang, Y., Roberts, J. A., Huber, M. A., Yao, H., Shi, X., Bechtel, H. A., Gilbert Corder, S. N., Heinz, T. F., Zheng, X., Fan, J. A. 2022. *ACS Nano*, just accepted. https://doi.org/10.1021/acsnano.1c10489

[2] Yao, Z., Chen, X., Wehmeier, L., Shao, Y., Zeng, Z., Liu, F., McLeod, A., Gilbert Corder, S., Tsuneto, M., Xu, S., Shi, W., Wang, Z., Zheng, W., Bechtel, H., Carr, G., Martin, M., Zettl, A., Basov, D., Chen, X., Eng, L., Kehr, S., Liu, M. 2021. *Nat. Comm.* 12, 2649. https://doi.org/10.1038/s41467-021-22844-3

Tip-enhanced infrared nanospectroscopy of proteins in individual lipid membrane patches and extracellular vesicles

Valeria Giliberti[1], **Raffaella Polito**[2], **Maria Eleonora Temperini1**[1,2], **Ljiljana Puskar**[3], **Ulrich Schade**[3], **Leonetta Baldassarre**[2], **Michele Ortolani**[2]

1. Istituto Italiano di Tecnologia, Center for Life Nano- & Neuro-science, Rome, 00161 Italy
2. Department of Physics, Sapienza University of Rome, 00185 Italy
3. Helmholtz-Zentrum Berlin für Materialien und Energie GmbH, Berlin, 12489 Germany

E-mail: valeria.giliberti@iit.it

Tip-enhanced infrared (IR) nanospectroscopy methods combine high resolution atomic force microscopy (AFM) with IR spectroscopy, pushing at the nanoscale the well-known label-free sensitivity of IR spectroscopy to chemical bond orientation and length. These methods represent a promising approach to perform functional studies of biomolecules with nanometer lateral resolution, thereby approaching the single molecule limit within inhomogeneous, crowded biological environments, in a fluorescent-label-free fashion.

Here we apply tip-enhanced IR nanospectroscopy technique based on the photoexpansion effect (AFM-IR) to two distinct case studies: (i) individual lipid membrane patches embedding the photosensitive transmembrane protein channelrhodopsin (ChR) typically used for optogenetic applications, and to (ii) hundred-nanometer-sized microvesicles (MVs), extracellular vesicles generated by the outward budding of the plasma membrane, which represent a major frontier in pharmacology since they act as vehicles of RNA, proteins and bioactive lipids.

In order to probe the functional conformational changes of ChR we implemented the AFM-IR nanospectroscopy platform with a visible illumination setup (see Fig. 1a) so as to perform difference IR nanospectroscopy by acquiring the difference absorption spectra $\Delta A=A_{blue}-A_{dark}$ (visible light ON state-visible light OFF) [1, 2]. We probed relative absorption variations smaller than 10^{-2} down to individual 14 nm-thick membrane patches (Fig. 1b). Micro-FTIR difference spectroscopy results obtained on the same samples have been used to validate the AFM-IR difference spectra. The unprecedented sensitivity of 10^2 ChR molecules reached by AFM-IR in probing light-induced conformational changes opens the way towards the combination of IR spectroscopic capabilities with electrical probing at the nanoscale, which is also possible with AFM, and it is of crucial importance for transmembrane proteins.

For the second case study of MVs, we present the correlation of topographic, mechanical and spectroscopic information that allowed us to identify two main populations of MVs in the same sample of cell culture medium. The two populations featured different chemical cargo suggesting different functions [3]. MVs from the first population are rather uniform, while MVs from the second population display a "soft spot" at their interior which we identify with protein-aggregate cargo. In Fig. 1c we report AFM-IR nanoimaging and nanospectroscopy data from an individual MV belonging to the second population: the entire map shows the vibrations of nucleic acid (here RNA at 1135 cm^{-1}), but only the soft spot displays the main protein absorption bands (amide I and II centered at 1660 and 1540 cm^{-1}, respectively).

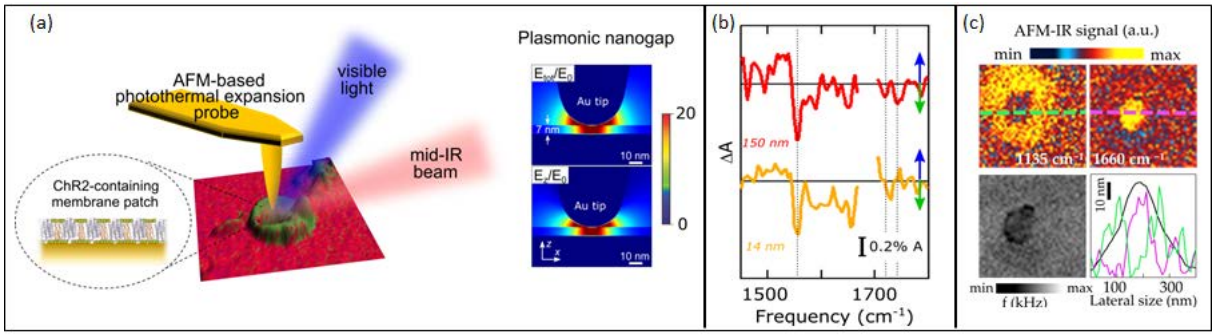

Fig. 1 (a) Sketch of the AFM-IR platform coupled to the visible illumination setup. Monolayer sensitivity is achieved by exploiting field enhancement in the plasmonic nanogap that forms between a gold-coated AFM tip and a gold surface used as sample support (see electromagnetic simulations on the right). (b) AFM-IR ΔA spectrum of ChR probed on a thick stack of lipid membrane patches (150 nm-thick) and on an individual lipid membrane patch (14 nm-thick). The positive and negative bands are related to conformational changes linked to the ion-channel activity of the protein. (b) Top: IR nanoimaging of an individual MV acquired at the main absorption band of RNA (1135 cm^{-1}) and of proteins (1660 cm^{-1}). Bottom left: map of the mechanical resonance of the AFM cantilever in contact with the sample (*f*); bottom right: topography line-scan (black) and AFM-IR signal line-scan acquired along the green (pink) dashed line in the AFM-IR map acquired at 1135 cm^{-1} (1660 cm^{-1}).

References

[1] Giliberti, V., Polito, R., Ritter, E., Broser, M., Hegemann, P., Puskar, L., ... & Ortolani, M.. 2019. *Nano Letters*, 19 (5), 3104-3114.
[2] Polito, R., Temperini, M. E., Ritter, E., Puskar, L., Schade, U., Broser, M., ... & Giliberti, V. 2021. *Phys Rev Appl*, 16 (1), 014048.
[3] Polito, R., Musto, M., Temperini, M. E., Ballerini, L., Ortolani, M., Baldassarre, L., ... & Giliberti, V. 2021. *Molecules*, 26 (4), 887.

Bridging atomic and reactor scales in plasmon catalysis for efficient, selective, and sustainable chemistry

Jennifer Dionne

Department of Materials Science and Engineering, Stanford University, Stanford, CA 94305, United States

jdionne@stanford.edu

Chemical manufacturing is critical for industries spanning construction, clothing, plastics, pharmaceuticals, food, and fertilizers, yet remains among the most polluting and energy-demanding practices. Our vision is to enable sustainable chemical production with atomically-architected photocatalysts that precisely control molecular interactions for high-efficiency and product-selective chemistry. Controlling photochemical transformations requires bridging the length-scale between a catalyst's atomic-scale structural features that influence dynamics and the macroscale extrinsic parameters that can be controlled (e.g., illumination, temperature, pressure). Optical excitation of plasmons offers a solution for overcoming this size mismatch - creating nanoscopic regions of high electromagnetic field intensity that can modify electronic and molecular energy levels, enable access to excited-state dynamics, and open new reaction pathways that are impossible to achieve under typical conditions. Further, plasmons can be efficiently excited with sunlight or solar-driven LEDs, for sustainable chemical transformations.

Here, we present our research advancing plasmon photocatalysis from the atomic to the reactor scale. First, we describe advances in in-situ atomic-scale catalyst characterization, using environmental optically-coupled transmission electron microscopy (OTEM). With both light and reactive gases introduced into the column of an electron microscope, we can monitor chemical transformations under various illumination conditions, gaseous environments, and at controlled temperatures, correlating three-dimensional atomic-scale catalyst structure with photo-chemical reactivity. Then, we describe how these atomic-scale insights enable optimized reactor-scale performance. As model systems, we consider two reactions: 1) acetylene hydrogenation with Ag-Pd catalysts and 2) CO2 reduction with Au-Pd catalysts. Here, Au/Ag acts as a strong plasmonic light absorber while Pd serves as the catalyst. We find that plasmons modify the rate of distinct reaction steps differently, increasing the overall rate more than ten-fold. Secondly, reaction nucleation occurs at electromagnetic hot-spots – even when those hot-spots do not occur in the preferred nucleation site. Finally, plasmons open new reaction pathways that are not observed without illumination, enabling both high-efficiency and selective catalysis with tuned bimetallic composition. Our results help elucidate the combined roles of optical, electronic and chemical contributions to plasmon photocatalysis, en-route to record efficiency and selectivity.

Electrically-connected antennas and nano-circuitry

Bert Hecht[1], **Monika Emmerling**[1], **Philipp Grimm**[1], **Sebastian Hammer**[2], **Rene Kullock**[1], **Jessica Meier**[1], **Maximilian Ochs**[1], **Jens Pflaum**[2], **Maximilian Rödel**[2], **Enno Schatz**[1,3], **Simon Wiegand**[2], **Stefan Zeißner**[1], **Luka Zurak**[1]

1. Nano-Optics & Biophotonics Group, Experimental Physics 5, University of Würzburg, Am Hubland, 97074 Würzburg, Germany
2. Experimentelle Physik 6, Universität Würzburg, Am Hubland, 97074 Würzburg, Germany
3. NanoStruct GmbH, Friedrich-Bergius-Ring 15, 97076 Würzburg, Germany

E-mail: hecht@physik.uni-wuerzburg.de

The electrical excitation of plasmonic nanoantennas and guided plasmonic modes at the nanoscale enables integration of subwavelength light sources and optical nanocircuitry into nano-opto-electronics. Inelastic electron tunneling proved to be a useful technique to convert electrons into plasmons enhanced via the local density of states in the antenna gap. We have employed this technique not only to demonstrate directed electrically-driven light emission [1] (see Fig. 1a) but also to excite selected modes in two-wire plasmonic nanocircuitry [2] (see Fig. 1b).

In order to increase the quantum efficiency of such devices it is a good idea to establish real transitions within the antenna gap. In a recent study we have therefore implemented an organic light emitting antenna whose emission characteristics can be switched by coupling the active material, zinc phthalocyanine (ZnPc), to antennas of different geometries by switching the charge carrier recombination zone [3].

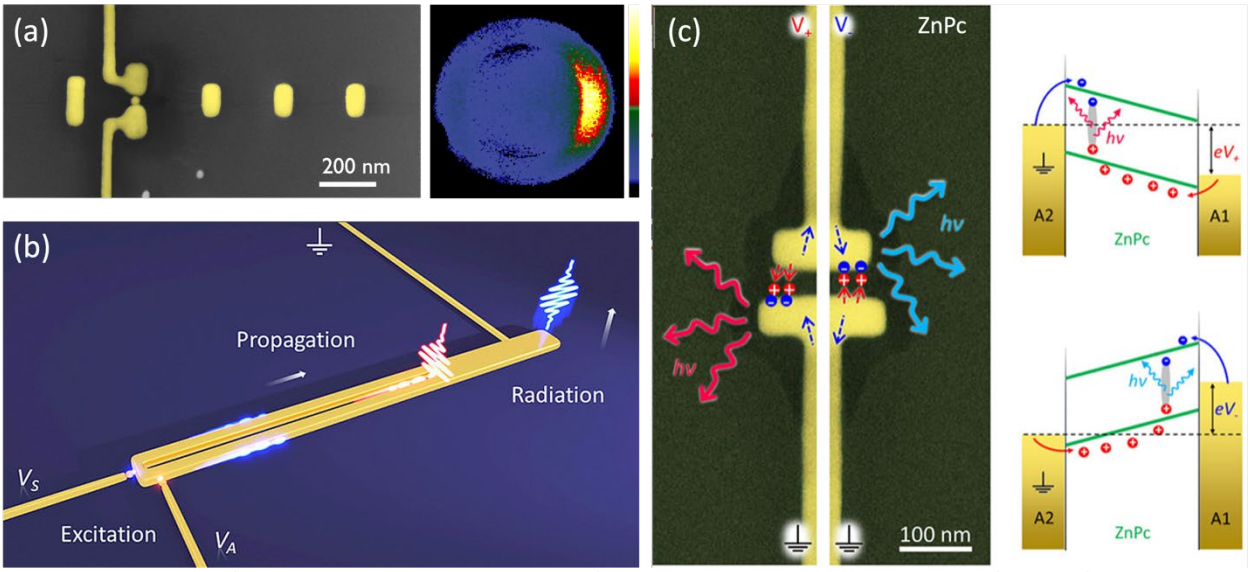

Fig. 1 Overview of electrically-connected plasmonics. (a) Left panel: Electrically-driven Yagi-Uda antenna fabricated from single crystal gold platelets. Right: Corresponding far-field emission pattern. (b) Artistic view of an electrically driven plasmonic nanocircuit featuring two tunnel junctions to selectively excite the modes of a two-wire transmission line. (c) Illustration of site-selective charge carrier recombination and corresponding antenna-enhanced light emission for positive (left panel) and negative (right panel) applied voltage to the upper antenna. Here, as ZnPc behaves as a preferential hole conductor, the recombination occurs at the cathode, i.e., the negatively charged antenna, which dictates the electroluminescence (EL) spectrum. Right-most panel: Schematic energy diagram of the Au/ZnPc/Au junction with applied voltage V illustrating the preferential hole conduction.

In this presentation we review the current status of electrically-connected nanoplasmonics and outline possible future directions.

References

[1] Kullock, R.; Ochs, M.; Grimm, P.; Emmerling, M.; & Hecht, B. Electrically-driven Yagi-Uda antennas for light, *Nature Commun.* 11, 115 (2020)
[2] Ochs, M.; Zurak, L.; Krauss, E.; Meier, J.; Emmerling, M.; Kullock, R.; & Hecht, B. Nanoscale Electrical Excitation of Distinct Modes in Plasmonic Waveguides, *Nano Lett.* 21, 4225-4230 (2021)
[3] Grimm, P.; Zeißner, S.; Rödel, M.; Wiegand, S.; Hammer, S.; Emmerling, M.; Schatz, E.; Kullock, R.; Pflaum, J. & Hecht, B. Color-Switchable Subwavelength Organic Light-Emitting Antennas, *Nano Lett.* 22, 1032-1038 (2022)

Polarization-sensitive near-field optical microscopy in the mid-infrared wavelength regime

Felix G. Kaps[1], Hamed Aminpour[1], Susanne C. Kehr[1], Lukas M. Eng[1]

1. Institute of Applied Physics, Technische Universität Dresden, 01062 Dresden, Germany

E-mail: felix_gregor.kaps@tu-dresden.de

Scattering scanning near-field optical microscopy (s-SNOM) is an excellent technique to study the optical, infrared and THz properties of materials on the nanoscopic scale. It is applied to various research fields e.g. 2D materials [1,2], semiconductors [3] material sciences [4], and biology [5]. Especially close to the sample's characteristic material resonances, both signal strength and sensitivity to the sample's properties are enhanced. Therefore, it becomes possible to probe minute changes of optical properties caused by e.g. local stress [6,7], molecular orientation [8,9], or local optical anisotropy [3]. Moreover, near-field examinations are strongly dependent on well-chosen polarization orientations of both incident and scattered beams. Consequently, separating the sample's near-field response along different directions is enabled while equally reducing unwanted scattering and interference effects e.g. when using cross-polarized illumination and detection scheme [10]. For non-resonant excitation, strongest field enhancement is mostly achieved by excitation of the out-of-plane component. In resonance, however, excitation polarization both perpendicular and parallel to the sample surface results in equally strong near-field responses [11, 12], hence enabling full polarization analysis on the nanometer length scale.

Here, we examine the polarization-dependent response of non-resonant (Au) and resonant (SiC) samples in the near-IR regime at ~10.6 µm via polarization-sensitive s-SNOM using a tabletop CO_2-laser. Alternating the incident linear polarization angle, we compare resonant and non-resonant sample responses via polarization analysis of the scattered near-field signature (see Fig. 1a). While signal strength strongly depends on the light's polarization for the non-resonant case, with no signal being measured for s-polarized illumination, resonantly excited samples yield a strong near-field signal at any linear polarization angle. Independently from the excitation polarization, lobe structures are observed at the near-field's polarization signature (see Fig. 1b,c). These lobes are confirmed by theory in combining the analytic dipole model for near-field interaction [13] and the Jones matrix algorithm [14] for consideration of the specific detection path. Comparing both experiment and simulation, we aim for a fundamental understanding of the polarizations influence on the near-field interaction and disentanglement of the near-field parallel and perpendicular components via spectral and polarization signatures.

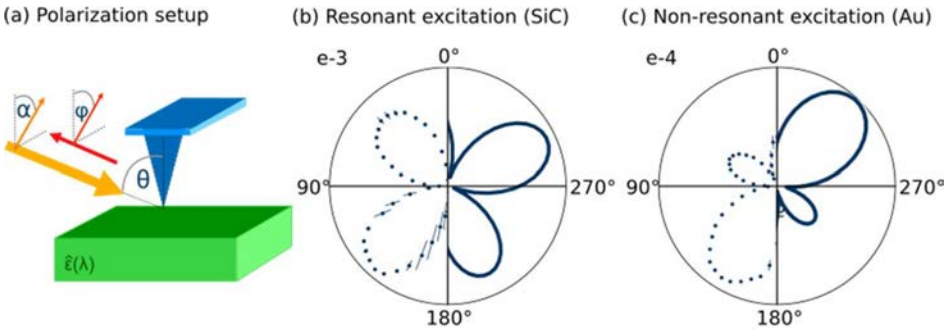

Fig 1: (a) Sketch of the polarization SNOM setup. (b,c) Polar diagrams of the near-field signatures on SiC (b) and Au (c) for incident polarization α=10° (at θ=60°) including experimental (light blue) and theoretical (dark blue) data. Different orientations of the polarization are observed as well as sidelobes in both cases. Notably, for the resonant case (SiC, b) the signal strength is about one order of magnitude higher compared to non-resonant excitation and the side lobes are characteristically increased, indicating stronger in-plane polarization states.

References

[1] J. Chen *et al.*, *Nature* 487, 77 (2012).
[2] de Oliveria, T.V.A.G., 2021, *Adv. Mater.*, 33, 2005777
[3] Ruta, F.L. et al, 2020, *Nano Lett.*, 20, 7933-7940
[4] Lang D. *et al.*, 2018, *Rev. Sci. Instrum.* 89, 033702
[5] Tucchin, V.V. , 2016, *J. Biomed. Opt.*, 21, 7
[6] Gigler, A.M. et al, 2009, *Opt. Express,* 17, 22351-22357
[7] Huber, A.J., et al, 2009, *Nat. Nanotech,*, 4, 153-157
[8] Mrkyvkova, N. *et al.,* 2021, *J.Phys. Chem.,* 125, 9229-9235
[9] Rao, V. J., *et al.*, 2020, *J. Phys. Chem.*, 124, 5331-5344
[10] Esslinger M., *et al.*, 2012, *Rev. Sci. Instrum.* 83, 033704
[11] Wehmeier, L. et al, 2019, *Phys. Rev. B*, 100, 035444
[12] Aminpour H., et al, 2020, *Opt. Exp.*, 28, 32316-32330
[13] Knoll B., Keilmann F., 2000, *Opt. Commun.* 182, 321
[14] Jones R. C., 1948, *J. Opt. Soc. Am.,* 38, 671

Colloidal Aluminum Nanoparticles for UV plasmonics

Jérôme Plain[1], Marion Castilla[1], Silvère Schuermans[1], Gil Markovich[2], Uri Hananel[2], Davy Gérard[1], Jérôme Martin[1], and Julien Proust[1]

1. L2n, UTT & CNRS ERL 7004, 12 rue Marie Curie 10004 Troyes Cedex, France
2. School of Chemistry, Tel-Aviv University, Tel-Aviv, 69978 Israel
E-mail: jerome.plain@utt.fr

Aluminum nanostructures appear as a good alternative to gold or silver because of the broad range of their plasmonic resonances (UV to NIR) and their reduced cost [1-2]. The main ways developed to obtain aluminum nanostructures are essentially based on top-down techniques (lithography's, laser ablation…).
Contrary to silver, these structures are very stable in air because with oxygen inclusion, a 3nm native passivation alumina layer is created and act as a protective layer. However, deterioration appears in a solvent for these structures [3].
Nevertheless, a lot of biological experiments occur in the UV range and aluminum nanostructures could help to enhance fluorescence detection. Consequently, it is of first importance to be able to work in organic solvents [4]. Consequently, the main objective is to synthesis colloidal aluminum nanoparticles with a tunable size and a sufficient stability in solvent in order to use them for biological sensing.

Based on sonochemistry and solvothermal reaction, we created a new way to synthesis aluminum nanoparticles in organic solvent with a short size distribution and a spherical appearance.
By varying controlled parameters, we can obtain different size with plasmonic responses in the UV range. The final aim is to do Metal-Enhanced Fluorescence of organic fluorophores for biological applications.

Acknowledgments : ANR SMFLUONA **(ANR-17-CE11-0036)**, Nano 'Mat, Région Grand Est, Feder funds are acknowledged for the financial support.

References

[1] Martin, J. Kociak, M. and al. 2014. *Nano lett.* 14,10, pp. 5517-5523

[2] Martin, J. Plain, J. 2015. *J. Phys. D. Appl.Phys.* 48: 184002

[3] Zhang, F. Proust, J. and al. 2017. *J. Phys. Chem. C*, 121, 13, pp. 7429-7434

[4] Akbay, N. Lakowicz, J.R. and Ray, K. 2012. *J. Phys. Chem. C*, 116, 19, pp. 10766-10773

Direct investigation of Anderson localization in topologically non-trivial photonic crystals

Sonakshi Arora[1], **Thomas Bauer**[1], **René Barcyzk**[2], **Ewold Verhagen**[2], **Kobus Kuipers**[1],

1 Kavli Institute of Nanoscience, Delft University of Technology, 2600 GA Delft, The Netherlands
2. Center for Nanophotonics, AMOLF, Science Park 104, 1098 XG Amsterdam, The Netherland
E-mail: s.arora@tudelft.nl

Topological photonics emulating the quantum valley Hall effect has recently gained attention due to its potential to offer immense control over optical signals and light-matter interactions stemming from a robustness against backscattering [1]. Recently, a concept for topological slow light devices has been put forward: a bearded topological photonic crystal interface supports a topological and a trivial mode around the K and K' valleys of the Brillouin zone [2]. This raises the interesting question whether or not the onset of Anderson localization caused by multiple scattering, which plagues slow-light applications in conventional photonic crystal architectures can be delayed or even avoided. Here we present a direct investigation of the onset of Anderson localization in topologically non-trivial photonic crystals with and without engineered disorder.

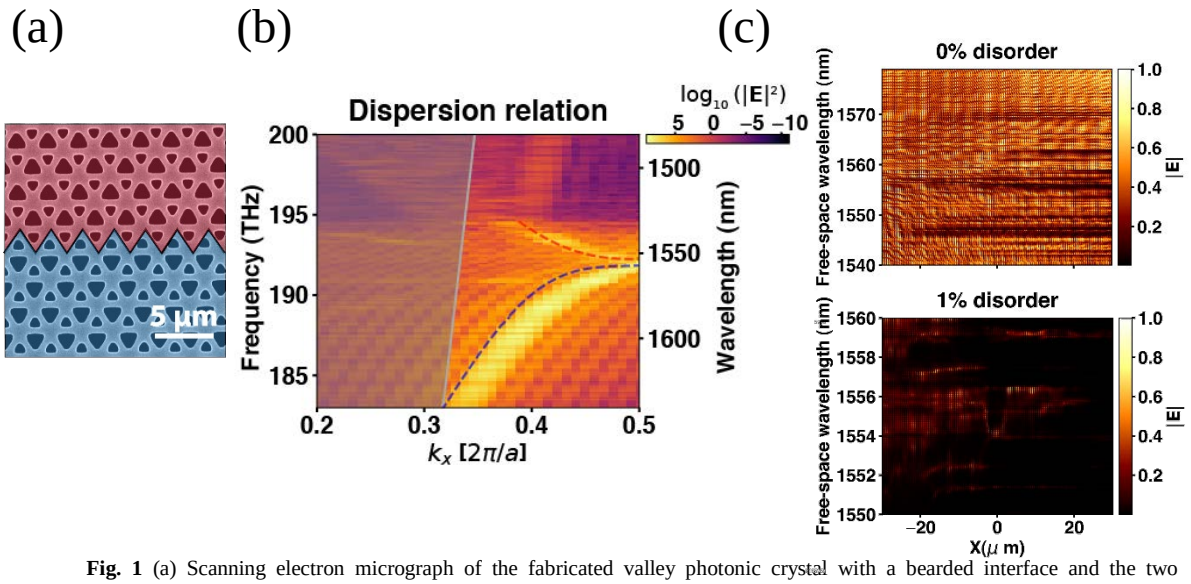

Fig. 1 (a) Scanning electron micrograph of the fabricated valley photonic crystal with a bearded interface and the two topologically distinct lattices on either side of the interface with pseudo colors. (b) Experimentally measured dispersion relation that shows the topological mode at lower excitation frequencies up to the crossing of the Brillouin zone edge, and the trivial mode at higher frequencies. The blue dashed curve is the numerically simulated dispersion of the topological mode, whereas the red dashed curve is the numerically simulated dispersion of the trivial mode. (c) Top image Electromagnetic field amplitude of photonic crystals with no intentionally induced disorders. Bottom image: Electromagnetic field amplitude of photonic crystals with 1% intentionally induced disorders that amount to 5nm random shifts of lattice sites.

We use amplitude- and phase-resolved near-field microscopy to visualize light propagation along the bearded interface (SEM shown in Fig. 1). We observe the photonic manifestation of Anderson localization, illustrated by the appearance of localized high intensity patches, only when we introduce engineered disorder in the structure. The real-space amplitude distributions as a function of frequency reveals different localized states that are associated with different quality factors. Using amplitude and phase-resolution we experimentally measure the two modes below the light cone in the dispersion relation and compare it with the numerical calculations (Fig. 1b). We quantitatively investigate a degree of merit called the backscattering mean free path (BMFP) for a range of geometrically engineered disorder and confirm that the BMFP falls with an increase in disorder.

More importantly, the experimentally determined BMFP for a topological vs trivial mode differs. This proves that the trivial mode within the same structures is more susceptible to spatial disorder than the topological mode.

References

[1] Lu, L., Joannopoulos, J. D., & Soljačić, M. (2014). Topological photonics. Nature photonics, 8(11), 821.
[2] Yoshimi, H., Yamaguchi, T., Katsumi, R., Ota, Y., Arakawa, Y., & Iwamoto, S. (2021). Experimental demonstration of topological slow light waveguides in valley photonic crystals. Optics Express, 29(9), 13441-13450.
[3] Rotenberg, N. & Kuipers, L. Mapping nanoscale light fields. Nat. Photonics 8, 919–926 (2014).

Disentangling cathodoluminescence spectra in dielectric nanoparticles: role of transition radiation

P. Elli Stamatopoulou[1], **Saskia Fiedler**[1], **Artyom Assadillayev**[2,1], **Christian Wolff**[1], **Hiroshi Sugimoto**[3], **Minoru Fujii**[3], **N. Asger Mortensen**[1,4], **Søren Raza**[2], **and Christos Tserkezis**[1]

1. Center for Nano Optics, University of Southern Denmark, Campusvej 55, DK-5230 Odense M, Denmark
2. Department of Physics, Technical University of Denmark, Fysikvej, DK-2800 Kongens Lyngby, Denmark
3. Department of Electrical and Electronic Engineering, Kobe University, Rokkodai, Nada, Kobe 657-8501, Japan
4. Danish Institute for Advanced Study, University of Southern Denmark, Campusvej 55, DK-5230 Odense M, Denmark

E-mail: elli@mci.sdu.dk

Electron-based microscopy techniques that harness signals generated from the excitation of a material by a fast electron beam have proven essential for exploring the optical properties of matter, and depending on signal nature and detection process, electron spectroscopy comes in different flavors. Among these, cathodoluminescence (CL) spectroscopy has been extensively employed for analyzing the near- and far-field in plasmonic and dielectric nanostructures [1].

Despite the success of CL spectroscopy in analyzing the optical response of various photonic nanostructures, such as the characterization of Mie-type resonances in nanoparticles, particular care must be taken when interpreting the CL measurements, since the recorded signal can originate from the interplay of different excitation mechanisms. Transition radiation (TR) is a prominent source of coherent electron-induced radiation emission, generated when the electron beam penetrates the nanoparticle [2]; as the electron approaches the surface of the particle, so does its image charge inside the medium, until, at contact, the two charges collapse, leading to the formation of an electric dipole. In spherical nanoparticles, two dipoles are created at the entrance and exit point of the electron beam that can interfere constructively or destructively (see Fig. 1a), depending on the electron time of flight inside the medium [3].

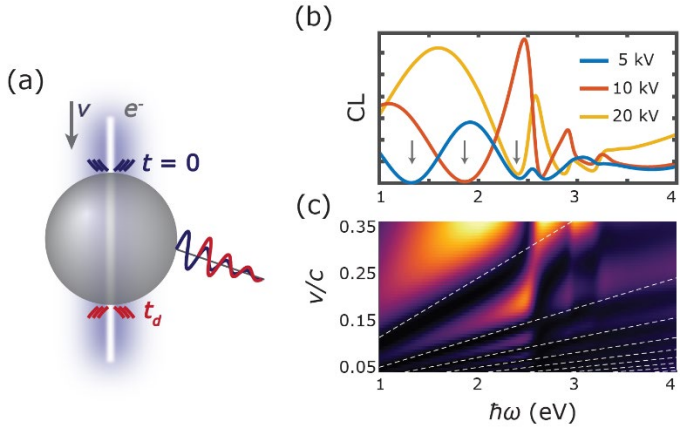

Fig. 1 (a) Emergence of TR at the upper and lower surfaces of a nanoparticle crossed by an electron beam through its center. The two waves interfere constructively or destructively, depending on the electron time of flight inside the particle. (b) Theoretical CL spectra for a silicon sphere 75 nm in radius, for the different acceleration voltages given in the inset. The arrows indicate the destructive interference minima. (c) Color map of the calculated CL spectra, as a function of the electron velocity. Thin white lines serve as guides to the eye for tracing the interference minima.

Here we discuss the emergence of TR and show, experimentally and theoretically, that interfering TR signals can generate distinct spectral features that distort the recorded spectrum (see markers in Figs. 1b and c) and lead to potentially erroneous assignment of modal characters to them. We develop a theoretical description that helps distinguish between the particle eigenmodes and the TR contribution. As an example, we focus on the case of silicon nanospheres, because of their high refractive index and low Ohmic losses [4], the multitude of co-existing modes in the visible [5], with the field largely confined inside the nanoparticle.

References

[1] García de Abajo, F. J. 2010. *Rev. Mod. Phys*., 82, 209–275.
[2] Yamamoto, N., *et al*. 1996. *J. Electron Microsc*., 45, 64-72
[3] Pogorzelski, R., and Yeh, C. 1973. *Phys. Rev. A*, 8, 137–144.
[4] García-Etxarri, A., *et al*. 2011. *Opt. Express*, 19, 4815–4826.
[5] Staude, I., *et al*. 2013. *ACS Nano*, 7, 7824–7832.

Nonlinear and quantum nano-optics with atomically-thin materials

Joel D. Cox[1,2]
1. Center for Nano Optics, University of Southern Denmark, Campusvej 55, DK-5230 Odense M, Denmark
2. Danish Institute for Advanced Study, University of Southern Denmark, Campusvej 55, DK-5230 Odense M, Denmark
E-mail: cox@mci.sdu.dk

Coherent optical control of light and atomic systems enables fundamental explorations of quantum physics while promising disruptive applications in diverse fields, ranging from information and communications technologies to optical sensing and metrology. In this context, the intrinsically strong and actively tunable light-matter interactions available in atomically-thin materials, such as graphene and ultrathin noble metals, offer unique opportunities to trigger nonlinear and quantum optical phenomena on the nanoscale by invoking their supported polaritons and/or near field interaction with proximal quantum light emitters [1]. Here we will discuss the excellent nonlinear response associated with 2D plasmon polaritons hosted by graphene [2], characterized by strong optical confinement and both electrical and mechanical tunability (see Fig. 1), as well as those manifesting in ultrathin crystalline noble metal films [3], with thickness-dependent properties and potentially lower losses than their amorphous counterparts. We shall then explore strategies to harness polariton-assisted nonlinear optical phenomena in 2D materials to resonantly couple with proximal quantum light emitters [4], mediate single-polariton-level nonlinear optical interactions on the nanoscale [5,6], and optically drive atomic systems into electrically-tunable bistable states.

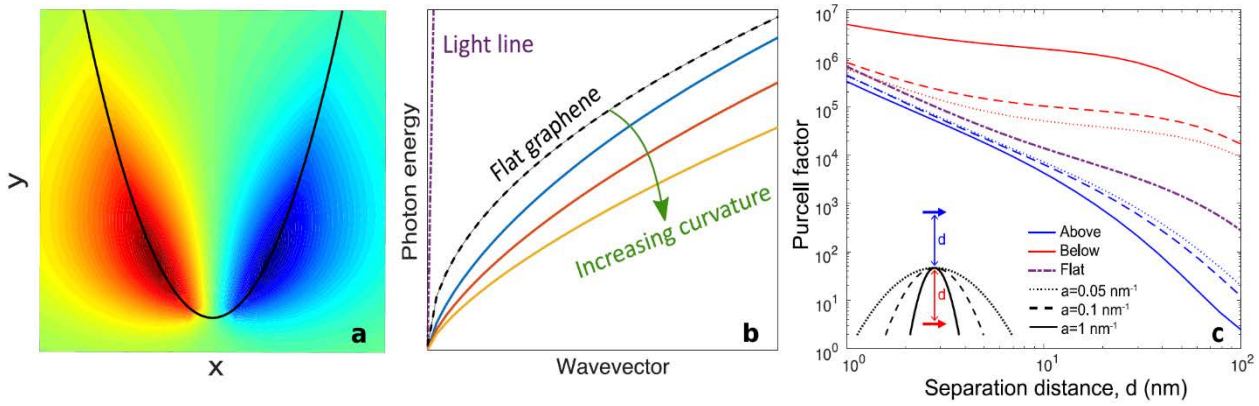

Fig. 1 Channel polaritons in parabolic two-dimensional waveguides. (a) Cross-section of the electric potential associated with the lowest-order plasmon mode supported by a parabolic graphene waveguide, formed by deforming a graphene sheet into a parabolic shape in the *x*-*y* plane to achieve both lateral and vertical field confinement. (b) Dispersion relation of polaritons in a 2D parabolic waveguide for different curvatures. (c) Purcell factor experienced by a quantum light emitter represented as a point dipole positioned at a distance *d* directly above (blue curves) or below (red curves) the parabola vertex, and oriented in the *x*-direction.

References

[1] Rasmussen, T. P., Gonçalves, P. A. D., Xiao, S. Hofferberth, S., Mortensen, N. A., and Cox, J. D. Polaritons in two-dimensional parabolic waveguides. ACS Photon. 2021, 8, 1840-1846.
[2] Cox, J. D. and García de Abajo, F. J. Nonlinear graphene nanoplasmonics. Acc. Chem. Res. 2019, 52, 2536-2547.
[3] Rodríguez Echarri, Á., Cox, J. D., Iyikanat, F., and García de Abajo, F. J. Nonlinear plasmonic response in atomically thin metal films. Nanophotonics 2021, 10, 4149-4159.
[4] Cox, J. D. and García de Abajo, F. J. Nonlinear atom-plasmon interactions enabled by nanostructured graphene. Phys. Rev. Lett. 2018, 121, 257403.
[5] Alonso Calafell, I., Cox, J. D., Radonjić, M., Saavedra, J. R. M., García de Abajo, F. J., Rozema, L. A., and Walther, P. Quantum computing with graphene plasmons. Npj Quantum Inf. 2019, 5, 37.
[6] Cox, J. D. and García de Abajo, F. J. Single-plasmon thermo-optical switching in graphene. Nano Lett. 2019, 19, 3743-3750.

Time-varying gradient metasurface with all-optical beam steering applications

Mohammad Karimi[1], **M. Zahirul Alam**[2], **Orad Reshef**[2], **Jeremy Upham**[2], **Robert Boyd**[2,3]

1. School of Electrical Engineering and Computer Science, University of Ottawa, Ottawa, Canada
2. Department of Physics, University of Ottawa, Ottawa, Canada
3. Institute of Optics, University of Rochester, Rochester, New York 14627, USA

E-mail: mkari094@uottawa.ca

The fast and large nonlinear optical response in epsilon-near-zero (ENZ) materials makes them perfect candidates for hosting all-optical, time-varying metasurfaces. Using a phase-gradient metasurface consisting of a plasmonic nanoparticle array fabricated over a thin layer of indium-tin-oxide (ITO), we demonstrate not only ultrafast control of the scattering fields, but also a clear asymmetry of this response in different scattering directions.

A phase-gradient metasurface is a 2D arrays of sub-wavelength scatterers that introduce coordinate-dependent phase response resulting in far-field sculpting of optical fields [1,2]. Figure 1(a) presents a schematic of our gradient metasurface. Each unit cell of the metasurface is made of four gold nanoantennas of varying length and the reflection phase of each antenna is a function of the length. The substrate is a 65-nm-thick ITO on glass. Due to the large nonlinear optical response of the antenna coupled ENZ media [3,4], a sufficiently strong femtosecond pump pulse modifies the reflection phase of each antenna by a different amount. This leads to adiabatic wavelength conversion (AWC) of a probe beam of light [5]. As a result of this conversion in the wavelength, the reflected diffraction orders (DO) steer to new angles. Figure 1(b) shows the schematic of the standard pump-probe set-up used for measuring the angular dispersion of the DOs of the probe in response to the presence of a pump. Figures. 1(c) and 1(d) show the angular distribution of the +1 and -1 DOs respectively, for different time delays between the pump and the probe. For co-incident pump and probe pulses, the DOs steer to new angles; a behavior that can be attributed to AWC. Of note, for identical pump and probe conditions, the +1 and -1 DOs show markedly different responses, with a factor of 2 difference in the shift of diffraction angle. The details of this discrepancy will be presented in the talk.

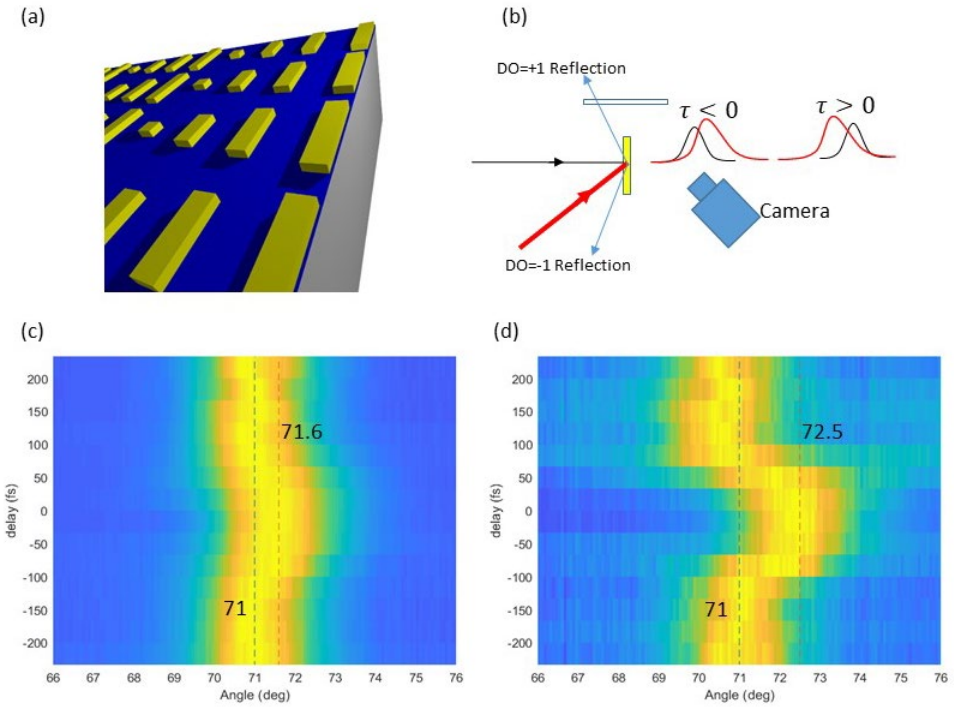

Fig. 1 (a) schematic of the gradient metasurface, (b) the simple schematic of the pump-probe set-up for measuring the angular distribution of the DOs, τ specifies the time delay between the pump and the probe beams, (c) and (d) the delay-dependent angular distribution of DO=+1 and DO=-1 respectively.

The authors acknowledge funding from the Department of National Defence's Innovation for Defence Excellence and Security (IDEaS) Program and DARPA.

References

[1] Genevet, P., et al., APL100, 013101 (2012).
[2] Sun, S., et al., APL 12, 6223–6229 (2012).
[3] Alam, M.Z. et al., Science 352, 795–797 (2016).
[4] Alam, M.Z. et al., Nature Photonics 12, 79–83 (2018).
[5] Zhou, Y. et al., Nature Communications 11, 1–7 (2020).

The case of nonlinear photoluminescence in plasmonics

Florian Dell'Ova[1], **Adrian Agreda**[1,2], **Deepak. K. Sharma**[1], **Konstantin Malchow**[1], **Gérard Colas des Francs**[1], **Erik Dujardin**[1] **and Alexandre Bouhelier**[1]

1. Laboratoire Interdisciplinaire Carnot de Bourgogne, CNRS UMR 6303, Université Bourgogne Franche-Comté, Av. A. Savary, 21000 Dijon, France

2. Laboratoire Photonique, Numérique et Nanosciences (LP2N), IOGS, Univ Bordeaux, CNRS, 1 Rue François Mitterrand, 33400 Talence France

E-mail: florian.dell-ova@u-bourgogne.fr

Upon absorption of an ultrafast laser pulse, metal nano-objects may create new up-converted photons by various plasmon-assisted nonlinear processes. Amongst them are well-known coherent mechanisms such as second or third harmonic generation. Another interesting nonlinear response is an incoherent effect traditionally referred as two-photon photoluminescence because of its (quasi)-quadratic dependence with the laser power and featuring a large emission spectrum spanning the visible to near-IR range.

The origin of this continuum remains debated in the literature with various hypothesis depending if one considers that the nonlinearity arises from the absorption (multi-photon transitions) or from the emission characteristics. Here we employ a more generic term for this mechanism: nonlinear photoluminescence or NPL.

In this work, we will present the different schools of thought and, supported on experimental data, we will highlight the role out-of-equilibrium electrons radiatively decaying and carrying the statistics of photon bunching [1]. We further show that the radiation is not only locally emitting photons at the laser excitation site but is exploring the entire body of the antenna [2]. We demonstrate that such a delocalized response is mediated by the underlying surface plasmon modal landscape, enabling thereby a polariton-mediated spatial tailoring and design of the nonlinear response [3]. We will discuss the possibility to engineer the spatial distribution of the surface plasmon modes to implement advanced functionalities such as logical gates [4].

Finally, we will conclude the presentation by showing how such nonlinear responses can be controlled on-demand by a static electrical command [5] as illustrated in Fig. 1 via a modification of the electron surface charge density.

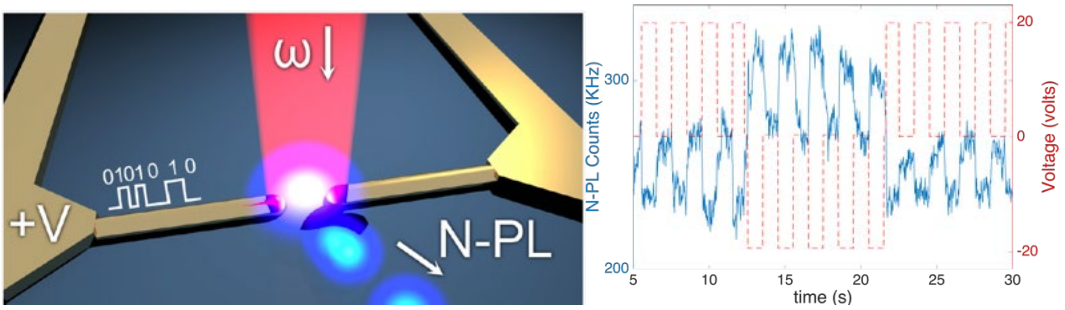

Fig. 1. Left: Illustration of the electrically controlled nonlinear photoluminescence (NPL) response of an optical gap antenna**.** Right: temporal trace showing a modulation of the NPL yield upon application of a square bias with two polarities. For positive voltage, NPL is quenched compared to null bias. For negative, N-PL is enhanced.

References

[1] K. Malchow et al., *Photon bunching of the nonlinear photoluminescence emitted by plasmonics metals,* J. Opt. Soc. Am. B, **38**, 576 (2021)
[2] A. Agreda et al. *Spatial distribution of the nonlinear photoluminescence in Au nanowires***,** ACS Phot. **6,** 1240 (2019)
[3] A. Agreda et al. *Modal and wavelength conversions in plasmonic nanowires***,** Optics Express, 29, 15366 (2021)
[4] U. Kumar et al. *Interconnect-Free Multibit Arithmetic and Logic Unit in a Single Reconfigurable 3 μm² Plasmonic Cavity,* ACS Nano **15**, 13351 (2021)
[5] A. Agreda et al. *Electrostatic Control over Optically Pumped Hot Electrons in Optical Gap Antennas,* ACS Phot. **7,** 2153 (2020)

Tunable vibrational nonlinear response in monolayer hBN

Fadil Iyikanat[1], **A. Konečná**[1], **F. Javier García de Abajo**[1,2]

1. ICFO-Institut de Ciencies Fotoniques, The Barcelona Institute of Science and Technology, 08860 Castelldefels (Barcelona), Spain
2. ICREA-Institució Catalana de Recerca i Estudis Avançats, Passeig Lluís Companys 23, 08010 Barcelona, Spain
E-mail: fadil.iyikanat@icfo.eu

Investigating nonlinear optical effects that occur during the interaction of light with materials at the atomic level is important for opto-electronic applications based on nanomaterials. Using first-principles calculations, we investigate the nonlinear optical response of monolayer hBN and demonstrate the plausibility of electrical tunability of vibrational modes with potential application in opto-electronics within the mid-infrared phonon-polariton region [1].

We proceed by first obtaining the potential energy surface and induced dipole density as a function of atomic positions. Then, solving the equation of motion either in the time domain and in a perturbative scheme, we obtain the nonlinear susceptibilities associated with second- and third-harmonic generation, as well as the Kerr effect. Besides the strong nonlinear response that situates this material on par with graphene as the most nonlinear materials in the mid-infrared region, we foresee that substantial frequency shifts exceeding the spectral widths of the phonon-polariton modes can be realized by applying in-plane DC fields that are attainable using existing lateral gating technology. We also predict quantum blockade at the few-quanta level in nanometer-sized hBN structures, with potential application in quantum technologies.

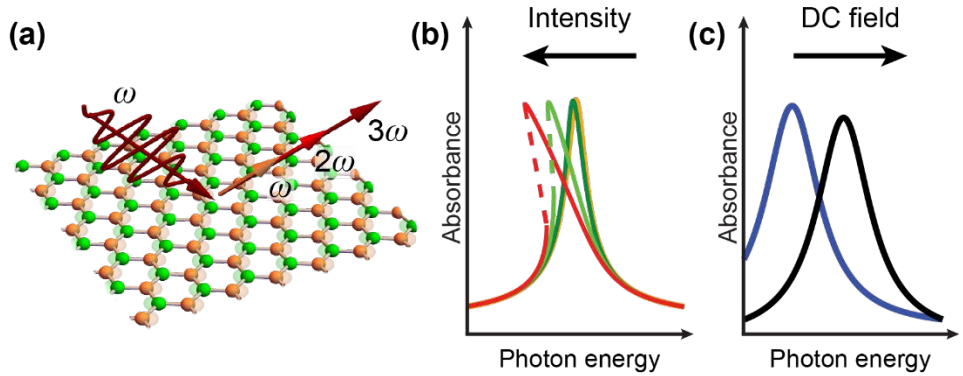

Fig. 1 (a) Illustration of monolayer hBN under normally impinging light irradiation with linear polarization along one of the B-N bond directions. (b,c) Spectral dependence of the absorbance for (b) increasing light intensity and (c) an applied DC field.

In summary, our work demonstrates that phonon polaritons in monolayer hBN with strong nonlinear response, long lifetime, and optical and electrical modulation configure a promising, robust platform that opens new possibilities in mid-infrared nonlinear optics with application in opto-electronics and quantum optics.

References

[1] Iyikanat, F., Konečná, A., and García de Abajo, F. J. 2021. Nonlinear tunable vibrational response in hexagonal boron nitride. *ACS Nano*, 15 13415-13426.

Acknowledgments; This work has been supported in part by the European Research Council (Advanced Grant 789104-eNANO), the Catalan CERCA Program, and Fundaciós Cellex and Mir-Puig.

Second harmonic generation under doubly resonant lattice plasmon excitation

Sebastian Beer[1], Jeetendra Gour[1], Alessandro Alberucci[1], Uwe Zeitner[1,2], Stefan Nolte[1,2]

1. Institute of Applied Physics, Friedrich Schiller University Jena, Albert-Einstein-Str. 15, 07745 Jena, Germany
2. Fraunhofer Institute for Applied Optics and Precision Engineering IOF, Albert-Einstein-Str. 7, 07745 Jena, Germany

E-mail: s.beer@uni-jena.de

The collective oscillations of free electrons in metals (plasmons) lead to a localized field enhancement at the surface, which can boost nonlinear optical effects. Accordingly, the behavior of metasurfaces with periodically arranged metallic nano-particles is dictated by two distinct plasmonic resonances: i) the localized surface plasmon resonance (LSPR) dependents only on the individual nanoparticles; ii) the surface lattice resonance (SLR), driven by the collective response of the periodic arrangement. The conditions for SLR are closely related to the presence of a diffraction mode propagating along the lattice, also known as Rayleigh anomaly (RA) [1]. Due to their higher quality factor Q, SLRs enhance the nonlinear response much more than LSPR. As a matter of fact, second harmonic generation (SHG) is maximized when either the fundamental frequency [2-4] or the second harmonic [5] is coupled to the SLR. Recently, the relevance of double-resonance in the presence of SLRs has been stressed out theoretically [6] and experimentally demonstrated by tilting the metasurface along two orthogonal directions [7]. At a specific incident angle and period, the double-resonance can be also achieved by tilting the metasurface just in one direction.

For this purpose, an experimental parametric investigation of the SHG on gold nanobars of fixed shape and periodically arranged in two-dimensional rectangular arrays [see Fig. 1(a)] was carried out. In our study we varied the lattice periodicity, the incidence angle, and the direction of the linear polarization. Figure 1(b) shows the angular dependence of the transmitted SHG signal for different periods (horizontal axis) when illuminating the metasurface with an ultrashort TM-polarized laser pulse (pulse duration 200 fs, wavelength 1032 nm). The conversion efficiency is significantly enhanced at the RA conditions (superimposed lines) at either the fundamental (red) or its second harmonic (green). Our results confirm that the emitted second harmonic has a maximum in the double-resonant case, where a pair of RAs at the different wavelengths are crossing each other [sketched in Fig. 1(a)]. The close connection between the linear and the nonlinear response of the plasmonic metasurfaces has been theoretically confirmed using a nonlinear inverse scattering approach. Finally, due to the high quality of our samples and the exploitation of the double-resonance condition, we achieved a maximum average SHG power of 190 pW for an input average power of 180 mW. Such a comparatively large efficiency – in combination with the large input power – allowed the direct measurement of both the spatial profile and the spectrum of the generated second harmonic with standard equipment.

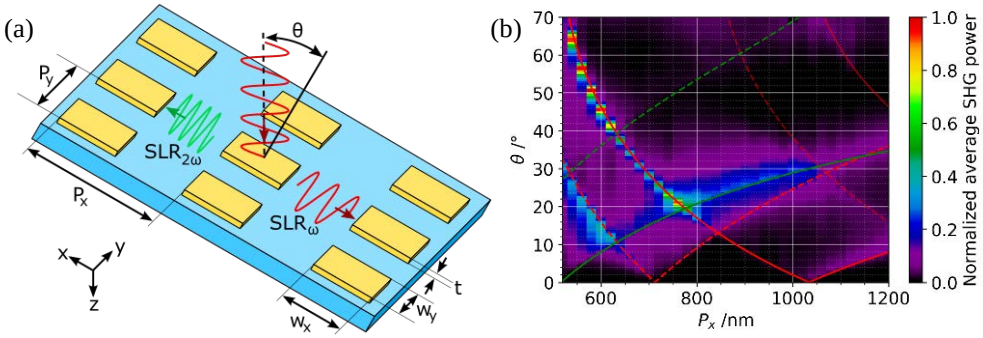

Fig. 1 (a) 2D lattice of gold nanobars on a 1 mm fused silica substrate. The geometrical parameters are $P_x \in [520\text{ nm}, 1200\text{ nm}]$, P_y=500 nm, w_x=400 nm, w_y=300 nm, t=50 nm. The double resonance case is qualitatively sketched, where the SLR takes place for both the wavelengths. (b) Normalized SHG power measured of the transmitted 0th diffraction order versus the lattice period and the incidence angle of the pump. The superposed lines show conditions where the RA is fulfilled (solid) in air and (dashed) in fused silica; the corresponding wavelengths are 1032 nm (red) and 516 nm (green).

References

[1] Kravets, V. G.; Kabashin, A. V.; Barnes, W. L.; Grigorenko, A. N. Plasmonic Surface Lattice Resonances: A Review of Properties and Applications. Chem. Rev. 2018, 118, 5912–5951.
[2] Czaplicki, R.; Kiviniemi, A.; Laukkanen, J.; Lehtolahti, J.; Kuittinen, M.; Kauranen, M. Surface lattice resonances in second-harmonic generation from metasurfaces. Opt. Lett. 2016, 41, 2684–2687.
[3] Hooper, D.; Kuppe, C.; Wang, D.; Wang, W.; Guan, J.; Odom, T.; Valev, V. Second Harmonic Spectroscopy of Surface Lattice Resonances. Nano Lett. 2018, 19.
[4] Klein, M. W.; Wegener, M.; Feth, N.; Linden, S. Experiments on second- and thirdharmonic generation from magnetic metamaterials. Opt. Express 2007, 15, 5238–5247.
[5] Michaeli, L.; Keren-Zur, S.; Avayu, O.; Suchowski, H.; Ellenbogen, T. Nonlinear Surface Lattice Resonance in Plasmonic Nanoparticle Arrays. Phys. Rev. Lett. 2017, 118, 243904.
[6] Huttunen, M. J.; Reshef, O.; Stolt, T.; Dolgaleva, K.; Boyd, R. W.; Kauranen, M. Efficient nonlinear metasurfaces by using multiresonant high-Q plasmonic arrays. J. Opt. Soc. Am. B 2019, 36, E30–E35.
[7] Stolt, T.; Vesala, A.; Rekola, H.; Karvinen, P.; Hakala, T. K.; Huttunen, M. J. Multiply-resonant second-harmonic generation using surface lattice resonances in aluminum metasurfaces. Opt. Express 2022, 30, 3620–3631.